# 2017 Annual Report

## Indo-Korea Science and Technology Center

# Contents

# Foreword

After 2014, the Indo-Korea Science and Technology Center (IKST) successfully changed its focus from scientific business to scientific research through internal research activities and collaborative projects with Indian researchers. We published a biannual report regarding our achievements in 2015–2016. We are now releasing an annual report for 2017 in an electronic document.

IKST has focused on three major research areas. First, we have been developing a platform for computational materials science. The Comprehensively Integrated Environment for Materials Simulation (CINEMAS) platform is planned to have a public release as a freeware before the first half of 2018. The development of this software is anticipated to be the central achievement of the IKST. The software is expected to be used by computational materials scientists, students, and professors. The second research area involves developing theories or source codes for material simulations. We have developed source codes for calculating the activation barrier of materials, predicting the atomic configurations of multicomponent alloys, and predicting the fatality of patients through machine learning techniques. We have also developed other small codes and tools. The third research area involves developing a descriptor of the catalytic activity of magnetic materials and suggesting a quantum phase transition for 3D bulk materials. The details are summarized in the following sections.

Along with research activities, we also put our efforts to develop a research network in India. Initially, we began our collaboration with the Jawaharlal Nehru Centre for Advanced Scientific Research (JNCASR). We have now extended the research network to institutes such as Indian Institute of Technology Bhubaneswar (IIT BBS), Indian Institute of Science (IISc), Indian Institute of Technology Bombay (IITB), Christ University, and Loyola College, Chennai. This network helps Koreans and Indians to understand each other and will be the starting point for a bilateral collaboration between the two countries. IKST will make considerable effort to enhance this relationship and achieve a higher level of collaboration.

IKST encourages Indian students and researchers to visit the Republic of Korea and has begun offering a visiting program to the Korea Institute of Science and Technology (KIST), Seoul, since 2018 as a part of the networking program. We look forward to having enthusiastic students and researchers participate in our program.

We are confident that these activities can enhance scientific achievements and promote research collaborations between the two countries.

**Dr. Seung Cheol Lee**

Director of IKST

## Introduction

The **Indo-Korea Science and Technology Center (IKST)** is a research organization located in Bengaluru, India. The center was established by the **Korea Institute of Science and Technology (KIST)** and inaugurated by **Dr. A. P. J. Abdul Kalam,** the former President of India, in January 2010.

The main objective of IKST is to build a **global knowledge platform (GKP)** between India and Korea in the area of science and technology. To achieve this, the IKST performs various activities.

- Collaborative research with Indian and Korean scientists and institutes
- Integrated R&D software platform development
- Indo-Korea researchers exchange programs
- Joint workshops and seminars with relevant scientists and institutes
- Survey research for specific topics

IKST aims to strengthen collaborations between Indian and Korean scientists by leveraging the complementary strengths and expertise of the two countries. IKST visualizes itself as a platform to aid advancements in the fields of science and engineering and develop next-generation technologies for the common benefit of the two countries.

Currently, IKST is located in Jakkur, Bengaluru, with a small R&D team in the area of Computational Materials Science and Machine Learning. IKST has partnerships with reputed Indian institutes, such as the Jawaharlal Nehru Centre for Advanced Scientific Research (JNCASR), Indian Institute of Science (IISc), Christ University, Indian Institute of Technology Bhubaneswar (IIT BBS), and Indian Institute of Technology Bombay (IITB).

**KIST** is the first multidisciplinary research institute in Korea founded by the Government of Korea. It has contributed significantly to the economic development of the country, particularly during the years of accelerated growth in the 1970s and 1980s.

*Laboratory Buildings No. 0, 1, and 2 in Autumn, KIST campus, Seoul, Korea*

**KIST** was established in 1966 under the auspices of the Korean and US governments. Its headquarters is located in Seoul, Korea, and it has two domestic branches, in Gangneung and Jeonbuk. It also has two international branches, namely KIST Europe in Germany and IKST in India.

**KIST** was ranked by Reuters as the World's $6^{th}$ Most Innovative Research Institute for two consecutive years, 2016 and 2017. The KIST was ranked after HHSL (US), AEAEC (France), JSTA (Japan) and NIAIST (Japan).

**KIST** aims to improve the quality of life worldwide by concentrating its research capabilities on assuring high competitiveness in the Korean and world economies.

**Key research areas of the KIST** are as follows:

- Brain Science
- Biomedicine
- Green City Technology
- Post-Silicon Semiconductor
- Robotics and Media
- Materials and Life Science
- Fuel Cell
- Clean Energy
- Sensor Systems
- Hybrid Photoelectric Devices

**KIST** also offers several unique academic graduate-level programs for domestic and international students from its partner universities—UST and IRDA.

# History

### January 2010

Korea–India Cooperation Centre was inaugurated by Dr. A. P. J. Abdul Kalam, former President of India, in the presence of Dr. Ahn Byeong-man, Hon. Minister of Education, Science and Technology, Republic of South Korea; Dr. Min Dong-pil, Director of KRCF; Dr. Han Hong-taek, Director of KIST; Dr. Balaram, Director, IISc.; Dr. Balakrishnan, Associate Director of IISc; and Dr. Rajiv Sharma, Advisor and Head of International Cooperation, Department of Science & Technology, Government of India.



### October 2013

A memorandum of understanding (MOU) was signed with the International Center for Material Sciences , JNCASR, and KIST during Prof. C. N. R. Rao’s visit to Korea for cooperation in joint research projects, symposiums, and workshops.

### August 2015

IKST office shifted to a new independent facility at NCC Urban Windsor, Yelahanka, Bengaluru.

### December 2015

An MOU was signed with the Karnataka Science & Technology Promotion Society (KSTePS) to develop a GKP.

### September 2016

An MOU was signed with the Center for Digital Innovation (CDI), Christ University, Bangalore, for cooperation in the SW area.

### January 2017

Dr. Seung Cheol Lee was appointed as the head of the IKST by the President of KIST, Dr. Byeong Gwon Lee.

### September 2017

An MOU was signed with the University of Texas at the Dallas International Future Semiconductor Innovation and Commercialization Center (UTD InFUSION), Kukmin University, Seoul, to conduct collaborative research for developing a corrosion module of Comprehensively Integrated Environment for Advanced Materials Simulation (CINEMAS).

## Organization

- Director
  - Research
    - Computational Materials Science
    - Software Development
    - Machine Learning/Data Analysis
  - Administration
    - Accounts & External Affairs
    - Human Resources & Purchase
    - Logistics & PR

**Manpower chart 2017**

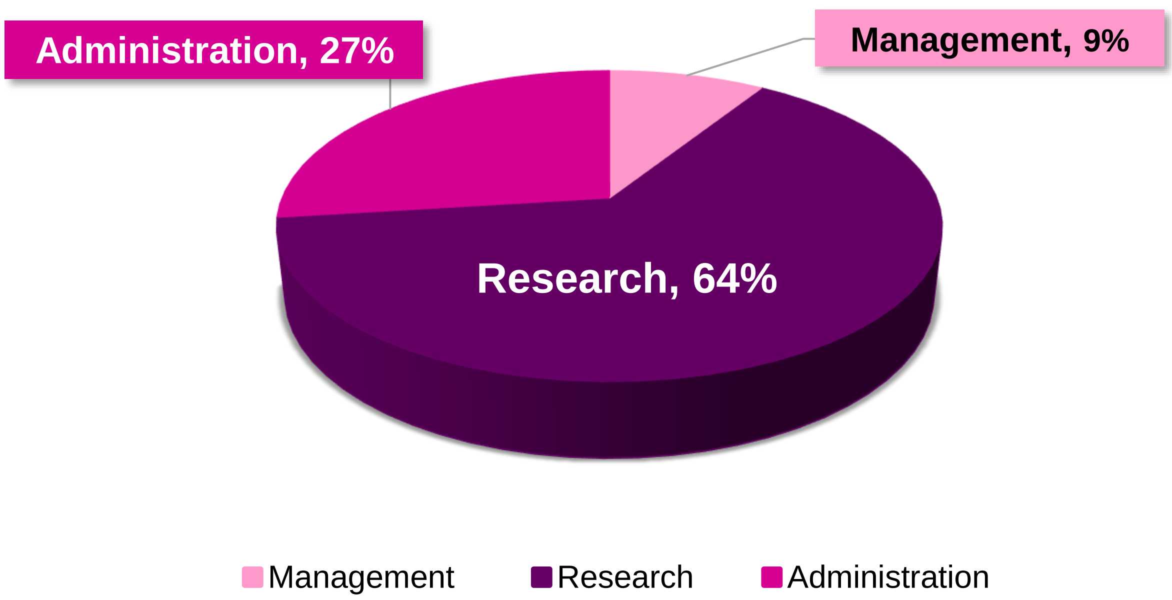

# LACOS: A Package for Atomistic Simulation of Solid Solution on a Lattice

**Mahesh Chandran**

Principal Research Scientist

**mahesh.chandran@ikst.res.in**

## Introduction

Most materials (metal and ceramics) that find applications are mixtures of more than two elements with their stoichiometries optimized to obtain a specific property target. In almost all cases, the materials are solid solutions, where the atoms are arranged on crystal lattice sites that seemingly appears to be disordered. The configuration does not possess any translational or rotational symmetry, but unlike amorphous materials, the atoms are on lattice sites with well-defined symmetries. Solid solutions can be contrasted with ordered crystalline materials, such as common salt (NaCl), in which atoms occupy well-defined positions on the lattice and are the same for all crystals. For such an ordered crystal, one can define a unit cell comprising a few atoms that can be periodically repeated in three-directional space to generate the bulk material. This also implies that for ordered crystalline material, all the fundamental material properties can be determined by studying the unit cell. For a solid solution, the absence of atomic ordering on the lattice means such a unit cell cannot be defined. Thus, in terms of the orderliness of atoms in materials, solid solutions fall in between fully ordered crystalline materials and completely disordered amorphous materials.

The current approach involves understanding and calculating material properties at atomic scales by using the density functional theory (DFT). Although very accurate, the DFT calculation is computationally intensive, which restricts its use to less than 100 atoms in most cases. For a solid solution, the absence of a unit cell implies that any property must be obtained by averaging it over all probable configurations. Performing such an average using direct DFT is computationally challenging and impractical, thus restricting its usage. Averaging also requires identifying the probable configurations, which by virtue of the Boltzmann factor ($e^{-E(\sigma)/k_B T}$) implies searching for low-energy configurations in a large configuration space[1].

Because direct DFT calculation is not practical, one resorts to creating a surrogate model for $E(\sigma)$. The model should satisfy the following two criterions: (*a*) the accuracy of energy should be as close to DFT as possible and (b) the computational cost of the model should be minimal (both time and memory). Such a model can be used to either directly enumerate all configurations (for a reasonable representation of the system) or can be combined with statistical approaches, such as Monte Carlo, to determine the "probable" low-energy configurations of the solid solution. Cluster expansion (CE) provides a similar approach [1, 2, 3]. CE uses clusters of lattice sites (also called figures) that are characterized by cluster correlation ($\overline{\Phi}$) as the basis set to represent any configuration dependent quantity. CE is today the state-of-the-art approach to model multicomponent solid solutions. A suite of computer codes called the Lattice Atomic Configuration Simulation (LACOS) package has been developed. The LACOS package uses CE to model multicomponent solid solutions. The essential features of this package are described in the following text.

## Cluster Expansion

The basic entity for CE is a cluster, which includes a set of lattice points and geometrical figures that can be used to represent the entire lattice. The occupation of a cluster by atoms is characterized using the cluster correlation function ($\Phi$) taken as a tensor product of the occupation variables (or point function of the occupation variables). A set of $\overline{\Phi}_\alpha$ forms an orthonormal basis set [1] that allows any configuration dependent quantity to be expanded in it. The expansion of configuration energy $E(\sigma)$ in this basis set is as follows:

$$E(\sigma) = \sum_{\alpha} J_\alpha \, \overline{\Phi}_\alpha(\sigma)$$

where the summation is over a set of clusters. $\{\alpha\}$ and $J_\alpha$ are the parameters of the model, which are also referred to as the effective cluster interactions (ECIs) because these terms

---

[1] *For a 100-atom system of binary alloy, there exist $2^{100}$ possible configurations. Even if one invokes lattice symmetries, the number of distinct configurations is still very large.*

are related to the average interaction between the atoms in the cluster (average is the overall configurations). The variable $\sigma$ represents the configuration of the system. The aforementioned equation can be used to calculate $E(\sigma)$ for an arbitrary configuration if the ECIs are known. To obtain the ECIs, one first solves the inverse problem by using a set of $E(\sigma)$ calculated using the DFT for some known configurations. Once the ECIs are known, the finite temperature ($T$) properties can be obtained by performing the Monte Carlo simulation.

An important aspect of the practical implementation of the CE method is the set of clusters that must be used for the expansion. The set of all clusters in a lattice grows exponentially with the size of the lattice. Therefore, keeping all the clusters in the expansion is computationally impractical. This led to the development of various methodologies for cluster selection coupled with solving the inverse problem, including the systematic search method [4], heuristic genetic algorithm (GA) [5], and simulation annealing [6]. In recent years, the sparse feature selection method has been used to build CE model [7]. The method is based on solving the following linear equation:

$$\min\|\mathbf{x}\|_p \text{ such that } \|\mathbf{y}-\mathbf{A}\mathbf{x}\|_2 < \epsilon$$

where $\|\mathbf{x}\|_p$ is the $p$-norm. Sparsity is enforced by using $p$ = 0 and 1. The advantage of this approach is that the aforementioned equation can be solved for an under-determined equation and has a unique sparse solution if the matrix $\mathbf{A}$ satisfies the property of restricted isometry. Solving an under-determined equation reduces the computational cost required for creating the set of DFT energies.

## LACOS – A suite of codes for CE

Based on all the recent developments, a suite of codes called the LACOS package has been implemented to build the CE model for a multicomponent solid solution. The basic framework of LACOS is displayed in Figure 1. It consists of the following modules.

ConfMaker: This module helps to create a set of configurations for calculating $E(\sigma)$ using the DFT. It can create a symmetry-distinct random configuration. Moreover, if a set of clusters is provided, this module can also generate configurations such that the corresponding matrix of cluster correlation ($\mathbf{\Phi}$) has small mutual coherence. The module automatically creates the directory-tree structure with each configuration in an independent directory with input files for the popular DFT package—Vienna Ab initio Simulation Package (VASP).

DFTrunner: This code automates the generation of a DFT database. The directory-tree created by ConfMaker becomes an input for this module, which submits the calculation to a computing cluster in batches. The script automates calculation monitoring, checks for convergence (and resubmission, if required), and parses the outputs to create a database file (with prefix DBinfo*). The database is used for solving the inverse CE problem to obtain the ECIs and set of clusters.

PyClex: Python Cluster Expansion (PyClex) is a module used to build the CE model using the database generated by DFTrunner. The code can be used for multisite and multicomponent solid solutions. The best set of clusters $\{\alpha\}$ is obtained using model selection techniques. The various algorithms implemented in PyClex for model selection broadly fall into three categories.

- Heuristic techniques: The GA and modified GA for sparse model selection.
- Approximate $L_0$-minimization using "greedy" algorithms: Orthogonal matching pursuit (OMP), CoSaMP, and iterative hard thresholding (IHT).
- $L_1$-minimization for sparse model selection: LASSO, split Bregman method, iterative shrinkage-thresholding algorithm (ISTA), and convex optimization.

CPyMonC: CPyMonC is a Monte Carlo code to perform finite temperature simulation. The best $\{\alpha\}$ and $J_\alpha$ from PyClex are inputs for this code. The Monte Carlo simulation provides access to finite-$T$ configurations of the material system, thereby allowing various thermodynamic quantities to be calculated.

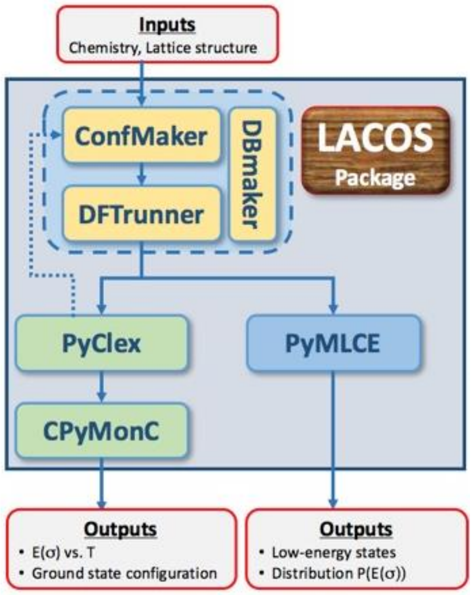


*Figure 1: Schematic of the framework of the LACOS package*

In addition to the described modules that aid the CE modeling of solid solutions, an additional machine learning (ML) module (PyMLCE) is also available. This module can be used to build a ML model of the configuration energy directly (see [8] for additional details). The LACOS is written on Python, with core computing performed in C (parts that are compute-intensive) and OpenMP used for parallelization on shared memory. The Monte Carlo simulation follows the domain decomposition approach for parallelization [3]. The LACOS package is currently aimed at modeling bulk solid solutions, and in the future, will be expanded to include surfaces to address problems such as catalysts, surface electrochemistry, and near-surface alloys.

Currently, the LACOS package is undergoing testing and benchmarking. Limited runs have indicated that for binary alloys, an accuracy of 1–2 meV/atom can be achieved in the prediction of total energy. For multicomponent alloys, an accuracy of approximately 10 meV/atom can be achieved. A comparison between DFT energies and CE-predicted energies for the ternary Ni-Al-Ti system is displayed in Figure 2

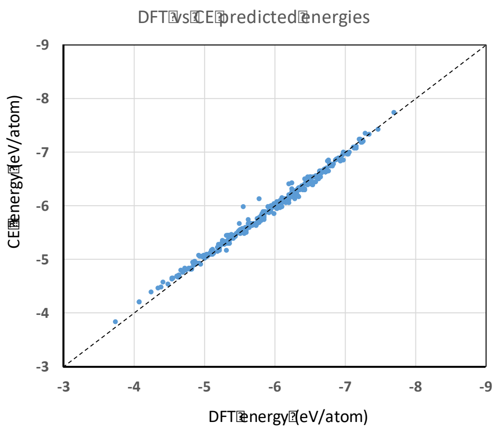


*Figure 2: Comparison of the DFT with CE-predicted energies for the Ni-Al-Ti system*

## Outlook

With the availability of a generalized CE code to model multicomponent solid solutions, this code would act as a potential bridge between first-principles calculation and higher length scale models. The package would also aid research in different aspects of industrially important alloys.

## References

1. J.M. Sanchez, F. Ducastelle, D. Gratias, *Physica* **128A**, 334 (1984)
2. D Lerch, O Wieckhorst, G L W Hart, R W Forcade and S Müller, *Modelling Simul. Mater. Sci. Eng.* **17**, 055003 (2009)
3. Mahesh Chandran, *Comp. Mat. Sci.* **108**, 192 (2015)
4. A. van de Walle and G. Ceder, *J. Phase Equilib.* **23**, 348 (2002)
5. G. L. W. hart, V. Blum, M. J. Walorski, and A. Zunger, *Nature Mat.* **4**, 391 (2005)
6. Mahesh Chandran (unpublished).
7. L. J. Nelson, G. L. W. Hart, F. Zhou, and V. Ozolins, *Phys. Rev. B* **87**, 035125 (2013)
8. Mahesh Chandran, S. C. Lee and J. H. Shim, *Modelling Simul. Mater. Sci. Eng.* **26**, 025010 (2018)

# CINEMAS: Latest Updates and New Features

**Kapil Gupta**

Research Scientist

**kapil.gupta@ikst.res.in**

## Introduction

CINEMAS is conceptualized as a graphical user interface (GUI)-based platform. CINEMAS handles calculations as graphical workflows with inbuilt tools, such as atomic visualizer and numeric plotter. These seamlessly integrated tools for analyzing the output data are tailored specifically for first-principle calculations. CINEMAS is being developed with the DFT as the main computational engine, but is not limited to it. CINEMAS also felicitates secondary calculations by using DFT outputs. A high-level concept of CINEMAS is represented in Figure 1. In this report, the latest updates on CINEMAS and its new features are explained.

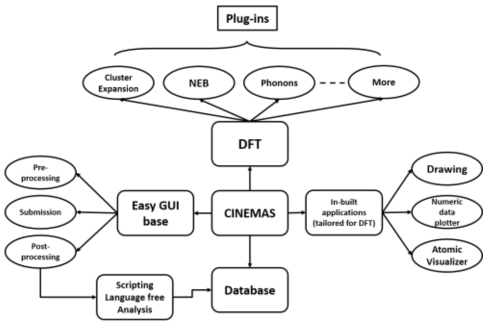


*Figure 1: Concept of CINEMAS*

## Latest Updates and Features

CINEMAS has been updated and stabilized extensively with respect to last year's developments. The new features added to CINEMAS are as follows.

## Conditional Jobs

Conditional jobs is a feature within CINEMAS where the user can define condition(s) on the output of a job and give instructions to the dependent jobs. This can be done even before the parent job is started. CINEMAS automates the execution of several mutually dependent jobs. Figure 2 represents one such example of computing the density of states (DOS) from a relaxation calculation. In this example, if the energy convergence (dE) reaches up to 0.00005 eV, CINEMAS will automatically copy the calculated relaxed structure (RS) as an input structure (IS) for the DOS calculation and execute it on the remote computer server. In the future, CINEMAS will have many such options for conditions and instructions to enhance the automation of calculation executions.

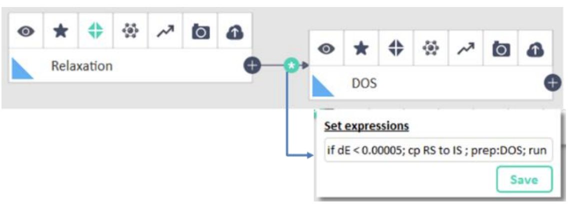


*Figure 2: Conditional jobs with automatic execution of calculations*

## Copy/Paste Feature for Jobs of a Similar Type

On CASCADE, the copy/paste option is now available in CINEMAS. This feature can be used to prepare workflows (calculations) of a similar type, with only a few parameters changed. For example (Figure 3), if the user has created one job with a particular value of energy cut-off, copy and paste can be performed to duplicate the workflow and only the cut-off value can be changed.

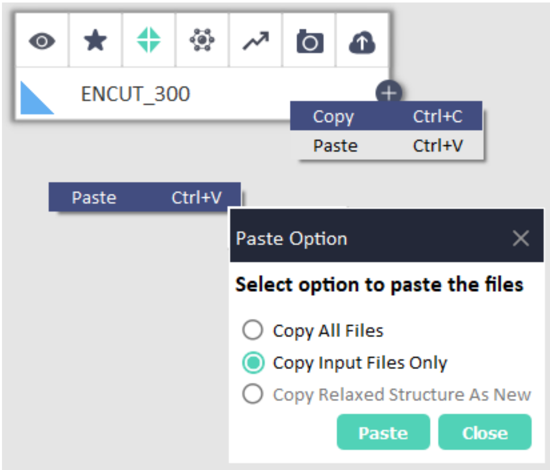


*Figure 3: Copy and paste option for calculations of a similar nature, with only a few parameters changed*

## Extended Volumetric Data Visualization

CINEMAS-view has extended its volumetric data capabilities. CINEMAS can now visualize many different sets of volumetric data, such as the electronic localization function (ELFCAR), partial charge density (PARCHG), and local potential (LOCPOT).

CINEMAS-view can now even add or subtract two sets of volumetric data with different grid sizes. Most of the available visualizers can add or subtract volumetric data within the same grid size. CINEMAS now has algorithms developed in-house for interpolations and performing addition or subtraction to match volumetric data with different grid sizes. This becomes very important because the user has to otherwise run the DFT again to obtain data with a similar grid size to perform the action.

## Automatic Detection of Files for Visualization

For a given calculation workflow, CINEMAS -view can now automatically detect all the files that can be visualized. Moreover, within the CINEMAS-view for single tabs corresponding to the workflow, the user can toggle between multiple files without opening many tabs. This essentially relieves the user from loading different files separately.

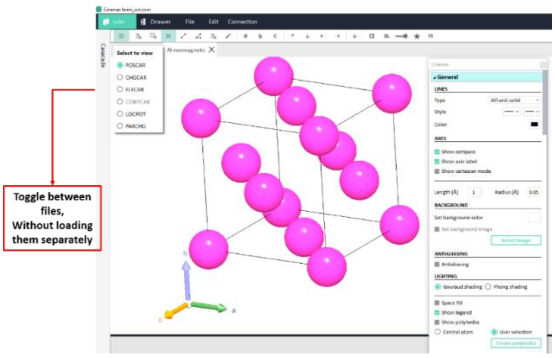


*Figure 4: Auto-detection of available files for visualization and easy toggle between views*

## Visualization of the Fermi Surface

CINEMAS-view can now visualize the Fermi surface for any given calculation. CINEMAS has a feature capable of visualizing the energy surface of bands crossing the Fermi level as well as that of other bands. CINEMAS has a very user-friendly interface to filter the data and for visualization. Within CINEMAS, individual bands and merged bands can be visualized within different settings, such as a reciprocal cell, unit cell, or in a Brillouin zone.

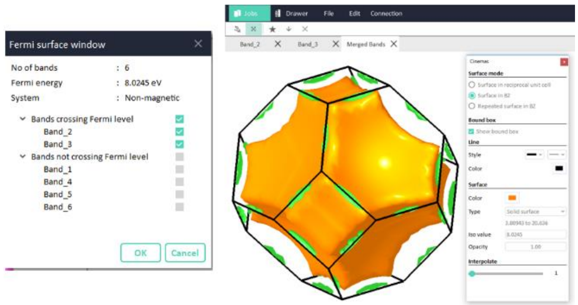


*Figure 5: Fermi surface, band selection, and visualization*

## Visualization of Forces on a Relaxed Structure

CINEMAS-view can now also visualize force vectors on atoms in a calculated structure. Apart from regular visual properties, the user can visualize the force vectors and also display the numerical value of a force vector by double-clicking on that vector (Figure 6).

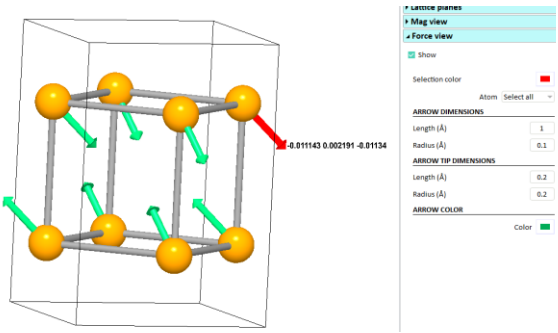


*Figure 6: Visualization of forces on a calculated structure*

## Visualization of the Magnetic Configuration of a Structure

CINEMAS-view can now also visualize the configurations for collinear as well as non-collinear magnetic orders. The user can easily toggle between the initial and calculated magnetic moments for a comparison. This feature enables the user to visualize different types of anti-ferro, ferro, or spin spiral magnetic orders.

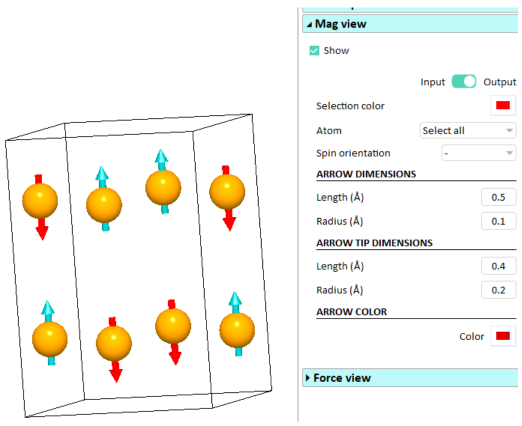


*Figure 7: Visualization of the magnetic order*

## Visualization of the Brillouin Zone of a Structure

When preparing the input files on a K-point preparation window, if a user intends to perform a band structure calculation, the user can visualize the Brillouin zone for the structure of any space group or geometry. The K-path can be selected and corresponding co-ordinates can be exported to the K-point input file (KPOINTS for VASP) (Figure 7).

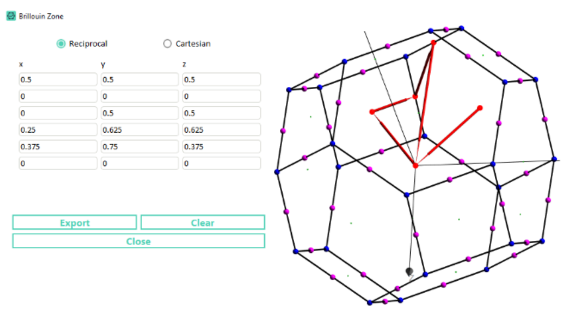


*Figure 8: Visualization of the Brillouin zone, selection of the K-path, and exporting of the coordinates*

## Structure Manager With Updated Miller Indices on-the-go

In addition to several features of the structure manager, a new feature of updating the Miller indices has been added to CINEMAS. When cleaving the surface of a particular Miller index from the bulk structure, the user has several choices for in-plane indices. Now, within the structure manager, a user can change and see the in-plane miller indices of the newly cleaved surface cell with a mouse click. Figure 8 illustrates the different choices for the in-plane miller indices of the <111> surface of a perovskite cell.

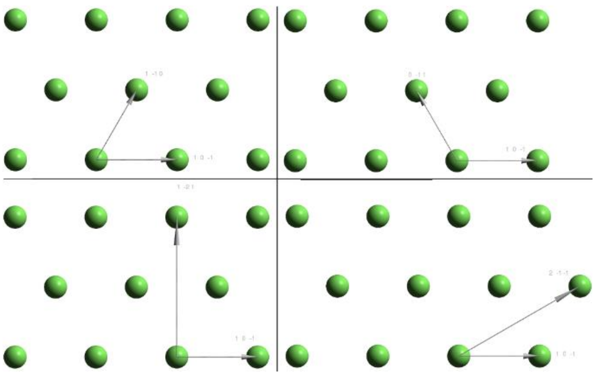

*Figure 9: Different choices for the in-plane Miller indices for a particular surface, with the dynamic display of changes*

The structure manager now has the following new features that are currently in the testing and stabilization stage:

1) Defining the degree of freedom for relaxation on different atoms by selecting layers. (selective dynamics for VASP).

2) Adsorption site detection on a surface for catalytic calculations: The structure manager can now automatically identify available adsorption sites for a particular surface, such as a bridge, hollow, or on-top. It can add an adsorbate from the available list in the structure manager.

3) Atoms can be replaced with any other elements, or an atom or molecule can be placed in the interstitial.

## Future Outlook

Curently, CINEMAS is only available for use in closed internal groups. The stable version of CINEMAS will soon be distributed for public use.

Users can register to access CINEMAS at https://www.ikst.res.in/download.php

Users can register on the CINEMAS user discussion forum at https://www.ikst.res.in/discussion-forum.php

For any query or information, please contact cinemas@ikst.res.in or kapil.gupta@ikst.res.in.

# First-Principles Studies of Energy and Functional Materials

**Satadeep Bhattacharjee**
Senior Research Scientist

**satadeep.bhattacharjee@ikst.res.in**

## Introduction

The major activities in first-principles-based modeling and simulation can be divided into the following categories:

1. **Energy materials:** In this field, we are working on catalysts for primarily electrochemical reactions. These works are mostly in-house activities. However, a few studies are underway in collaboration with researchers from Korea.
2. **Functional materials:** The current activities in this area include permanent magnets/hard magnets and III-IV semiconductors. These studies are mostly in-house activities in collaboration with researchers from Korea and India.
3. **Source codes:** We are developing certain ab-initio-based source codes in collaboration with theory and simulation groups in India. The codes are supposed to be integrated into the CINEMAS software [1].

In electrochemistry, we are studying the effect of magnetism on the chemical reactivity. These studies are motivated by the fact that most of the well-known catalysts are either 5d or 4d transition metals, such as Pt, Au, Ag, and Ir. These metals are expensive and scarce in nature. Therefore, designing the catalysts with cheap and abundant 3d transition metals and their oxides is beneficial. These materials are also environment friendly. In such materials, there exists another property, that is, magnetism that can be used to tune the catalytic activity. Bifunctional oxide catalysts are another group of materials that we are analyzing. Bifunctional catalysts are those that can be used in both oxygen reduction reactions (ORRs) and oxygen evolution reactions (OERs). Designing efficient catalyst beds is another area in which we are collaborating with researchers from KIST.

In the area of functional materials, we are working on permanent magnets, such as $Fe_2P$ and $F_{16}N_2$. Particularly, we have investigated the thermodynamic stability of these materials and obtained interesting results.

As already mentioned, we are developing source codes for studying transition states using the nudged elastic band (NEB). We are also employing the recently proposed automated nudged elastic band (Auto-NEB) method in collaboration with Prof. M. Jain of IISc, Bengaluru. Another code is being developed in collaboration with Prof. B. Muralidharan of IIT Bombay to study the transport in semiconductors.

A few highlights of the aforementioned studies are provided in the following text.

## Energy Materials

*Lowering the overpotential of ferromagnetic catalysts through spin orientation*

Oxygen-based electrochemical reactions are very important because they occur in fuel cells and metal oxygen batteries. In ORRs, nonmagnetic water is produced from paramagnetic oxygen molecules, whereas in OERs, paramagnetic oxygen molecules are produced from nonmagnetic water. These reactions are often very sluggish due to the over-binding of the reaction intermediates to the electrode surface. For example, if we consider the ORR mechanism in the cathode of proton-exchange membrane fuel cells [2,3] involves direct dissociation, the oxygen molecule ($O_2$) first undergoes a dissociative adsorption on the cathode, and then after subsequent reduction and protonation, the water is formed. The last two steps are very slow due to the over-binding of the reaction intermediates, such as O* and HO*, to the surface and require additional potential or overpotential to occur. This is a well-known issue [4,5] and several efforts have been made over the decades by tuning various parameters of the catalysts, which provides only a partial solution to the problem.

We studied whether there existed any magnetism-induced effect, which can decrease the overpotential. In particular, we studied if these reaction intermediates could be destabilized magnetically on the cathode surface such that these two steps could occur more easily.

By using FePd as a model electrode and the constrained DFT-based method, in which the relative orientation between the magnetization and the electrode surface can be controlled, we computed the free energies for different spin orientations and electrode potentials (Figure 1). Using this approach, we obtained the spin-dependent overpotentials. For the antiparallel spin arrangement between the surface and the adsorbate, the overpotential was approximately 0.43 V, whereas the overpotential was reduced by almost half for the parallel spin arrangement. In a real experiment, the reduction of overpotentials can be realized through the application of a weak electric field that polarizes the spins of the reaction intermediates in a manner that is unfavorable for strong chemisorptions, while simultaneously not affecting the magnetization of the electrode.

*Improving the performance of the bifunctional catalysts through doping*

Another group of activities in the domain of electrochemistry involves studying the effect of doping in bifunctional oxide catalysts with potential applications in unitized regenerative fuel cells. We investigated the double perovskite-based catalysts for bifunctional oxygen activity (OER and ORR) by using modified $Ba_{0.5}$ $Sr_{0.5}$ $Co_{0.8}Fe_{0.2}O_{3-6}$ (BSCF) and doping lanthanide ions ($Ln^{3+}$, $Nd^{3+}$, $Sm^{3+}$, and $Gd^{3+}$) into the A-site. Our study indicated that A-site doping had a significant effect on the bifunctional oxygen activity of double perovskite-based catalysts [7]. The oxygen activity of $NdBa_{0.5}$ $Sr_{0.5}$ $Co_{0.8}Fe_{0.2}O_{3-6}$ (NBSCF) was 0.973 V, which was much higher than that of previously reported transition-metal-based nanostructures.

## Functional Materials

*Role of zero-point effects in stabilizing the ground state structure of bulk $Fe_2P$*

The structural stability of bulk $Fe_2P$ was investigated in detail using first-principles calculations based on the DFT. While orthorhombic C23 phase is found to be energetically more stable, the experiments suggest it is a hexagonal C22 phase. The present study indicates that to obtain the correct ground state structure of $Fe_2P$ using first-principles-based methods, considering the zero-point effects, such as zero-point vibrations and spin fluctuations, is necessary. This study demonstrates one of the extremely rare situations in which a bulk material is stabilized by quantum effects that are important in 2D materials.

## First-Principle-Based Source Codes

*NEB and Automated NEB Module for DFT Codes*

Most chemical reactions are associated with energy barriers along the reaction pathway that hinder the spontaneity of the reaction. Changing the energy barrier along the reaction pathway allows one to manipulate the performance of a reaction. In this document, we present a module to calculate the energy barrier and locate the transition state of a reaction efficiently. The module is written in python and can perform NEB, climbing image NEB, and auto-NEB calculations. These methods require the knowledge regarding the potential energy surface and its gradient along some direction. This module is written such that it works in conjunction with DFT codes to obtain this information. Currently, the model is interfaced with three well-known DFT packages, namely VASP, Quantum Espresso, and Spanish Initiative for Electronic Simulations with Thousands of Atoms (Figure 2).

*Semiclassical transport module*

We developed a transport module based on the semiclassical Boltzmann transport equation. The module is written in python and can accept inputs from DFT codes, such as VASP. With a given set of inputs, the solution of the Boltzmann transport equation is obtained either through relaxation time approximation or numerically using the iterative method. The typical physical quantities that can be obtained from the calculations include the mobility, Seebeck coefficient, and figure of merit.

## References

1. https://www.ikst.res.in/cinemas.shtml
2. http://www.hydrogenics.com/technology-resources/hydrogen-technology/fuel-cells/
3. Hoogers, G. Fuel Cell Technology Handbook; Society of Automotive Engineers, U.S., 2003
4. Ralph, T. R.; Hogarth, M. P. Platinum Metals Review, 46, 3 (2002)
5. Larminie, J.; Dicks, A. Fuel Cell Systems Explained, 2nd ed.; JohnWiley and Sons Ltd: West Sussex, England, 2003
6. Satadeep Bhattacharjee and Seung-Cheol Lee, J. Phys. Chem. C, 2018, 122 (1), pp 894–901
7. Nam-In Kim, Rana Arslan Afzal, Sung Ryul Choi, Sung Won Lee, Docheon Ahn, Satadeep Bhattacharjee, Seung-Cheol Lee, Jung Hyun Kim, and Jun-Young Park, Journal of Materials Chemistry A, 25, 13019-13031 (201

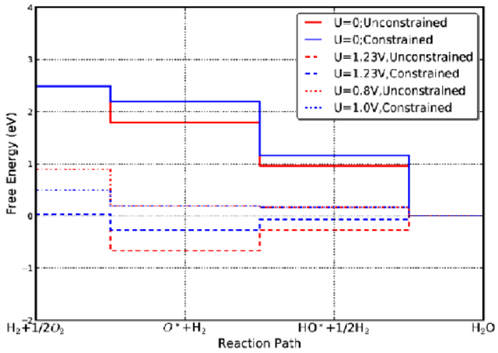


*Figure 1: Potential dependent free energy diagram for an ORR. The results are shown at zero potential (U = 0 V, solid lines), onset potentials (U = 1.0 and 0.8 V, dot dashed lines), and equilibrium potential (U = 1.23 V, dashed line). The blue (red) lines correspond (do not correspond) with (without) the constraints on the magnetic moments.*

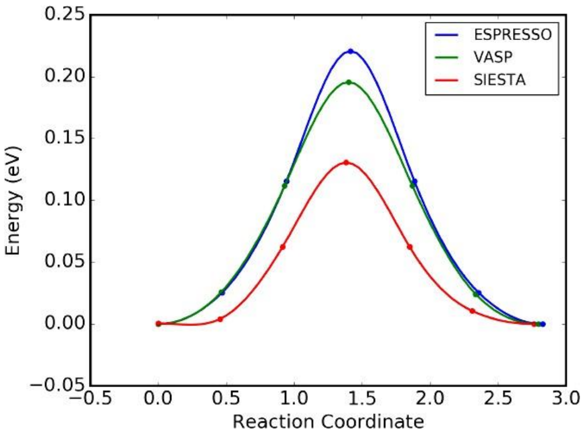


*Figure 2: Energy versus reaction coordinates plotted for the reaction $H_2$ + H -> H + $H_2$ using three DFT-based codes, as indicated in the inset*

# Functional Materials for Thermoelectric and Spintronic Applications

**Enamullah**
Research Associate

**enamullah@ikst.res.in**

## Introduction

Power crisis is one of the major global concerns and is rapidly growing. After the discovery of thermoelectricity by Seebeck and Peltier, people began thinking of methods to convert the residual (waste) heat into electricity because of high energy demands Direct conversion of the temperature gradient into electrical voltage is known as the Seebeck effect and the converse is known as the Peltier effect. The efficiency of thermoelectric materials depends on the transport coefficient of the constituent material in the following dimensionless figure of merit (*ZT*).

$$ZT = \frac{S^2\sigma}{k_e + k_l}T.$$

The figure of merit (*ZT*) is proportional to the Seebeck coefficient (*S*) and electrical conductivity ($\sigma$) and inversely proportional to the thermal conductivity ($k_e$ , $k_l$). A high value of *ZT* indicates a better candidate for thermoelectric applications. Therefore, for an efficient thermoelectric material, a high value of *S* and $\sigma$ and low value of *k* is required. However, according to the Wiedemann–Franz law (i.e., $k_e = L\sigma T$, where, $L$ is the Lorentz number), the electronic part of the lattice thermal conductivity is proportional to $\sigma$. Therefore, the optimization of *ZT* is a challenging task. Our aim is to investigate and search for various ways to reduce the lattice thermal conductivity, such as external doping and nanostructuring. The electronic band topology plays a crucial role in predicting efficient thermoelectric materials [1]. A sharp rise in the electronic DOS or a flat band near the Fermi level are the primary requirements for better transport and thermoelectric applications [1].

Spintronic research is based on the spin degree of freedom of electrons and is rapidly growing. It also has potential advantages over conventional electronics, such as high-speed data processing, low power consumption, and large circuit integration density [2]. Various materials, such as simple transition metal oxides ($CrO_2$, $Fe_3O_4$), perovskite manganites, transition metal chalcogenides, diluted magnetic semiconductors, and many Heusler alloys, are promising for spintronics applications [2, 3]. The striking feature of these materials is their half-metallic property. From the band concept, half-metallicity arises due to the existence of a finite DOS for one spin sub-band (majority channel) and a finite band gap for the other (minority channel) at the Fermi level. The imbalance in the two DOSs results in 100% spin polarization of conduction (majority) electrons at the Fermi level.

In the process of searching for functional materials for thermoelectric and spintronic applications, Heusler alloys [4] emerged as the most suitable candidate among all the others. Heusler alloys comprise a combination of transition metals (*d*-block) and nonmagnetic (*p*-block) elements. They exhibit a wide range of properties for various applications. For example, semiconducting property with a tunable band gap for solar cell applications, half-metallic for spintronic device applications, and semiconducting behavior for thermoelectric applications [4].

Apart from Heusler alloys, we are also actively involved in studying the transport properties of III-V semiconductors under various doping and strained conditions.

Some of the results of our research after joining the IKST are as follows.

## Research Project 1

Prediction of multifunctional quaternary Heusler alloys as promising candidates for spintronics and thermoelectric applications.

In this project, we predicted CoFeMnSb quaternary Heusler alloy as multifunctional for spintronic and thermoelectric applications [5]. The spin-polarized electronic structure analysis concludes the half-metallic characteristic, which consequently leads to 100% spin-polarized current (Figure 1). Apart from the half-metallic characteristics, the electronic band topology was found to be flat near the Fermi level, which characterized better transport properties for thermoelectric applications (Figure 2).

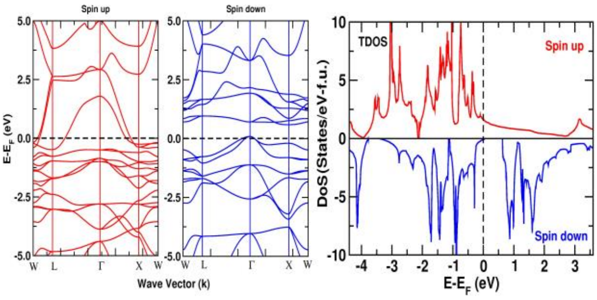


*Figure 1: Band structure (left) and spin-polarized electronic DOS (right) of CoFeMnSb. The half-metallic characteristics are revealed by the DOS plot.*

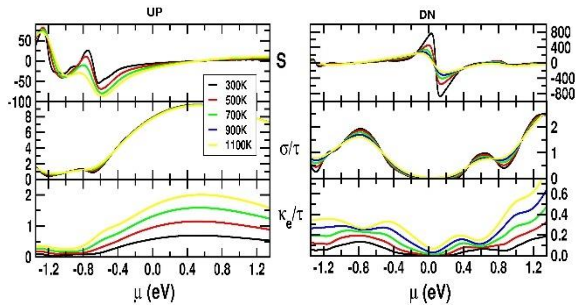


*Figure 2: Plot of various transport coefficients (S, $\sigma$, $k_e$) versus the chemical potential ($\mu$) for both spin up (UP) and spin down(DN) channels. The Seebeck coefficient (S) was measured in $\mu VK^{-1}$, electrical conductivity ($\sigma/\tau$) was $10^{20}$ $\Omega^{-1}m^{-1}s^{-1}$, and electronic part of the thermal conductivity ($k_e/\tau$) was $10^{16}$ $WmK^{-1}s^{-1}$.*

## Research Project 2

A defect-tolerant Heusler alloy for spintronic applications

This project is devoted to the study of one of the experimentally observed point defects, the antisite defect in the ternary $Co_2MnSb$ Heusler alloy. A theoretical analysis revealed that $Co_2MnSb$ is a highly efficient and defect-tolerant material for spintronic device applications [6]. We simulated the binary and ternary antisite disorders between transition metals and nonmagnetic elements up to the disordered concentration of 12%. Experimentally and theoretically, the antisite disorders considerably affected the half-metallic characteristics of the $Co_2$-based Heusler alloys [7, 8]. However, in our present case, we found that some of the disordered alloys preserved their half-metallic characteristics. In particular, the Mn-excessive and Sb-deficicent disordered alloys (e.g., $Co_2Mn_{1+x}Sb_{1-x}$, $Co_{2-x}Mn_{1+x}Sb$) preserve their half-metallic characteristics for all disordered concentration ($x$) with increasing magnetic moment [6]. Increasing magnetic moment leads to very high values of Curie temperature, which is another prerequisite for spintronic device applications.

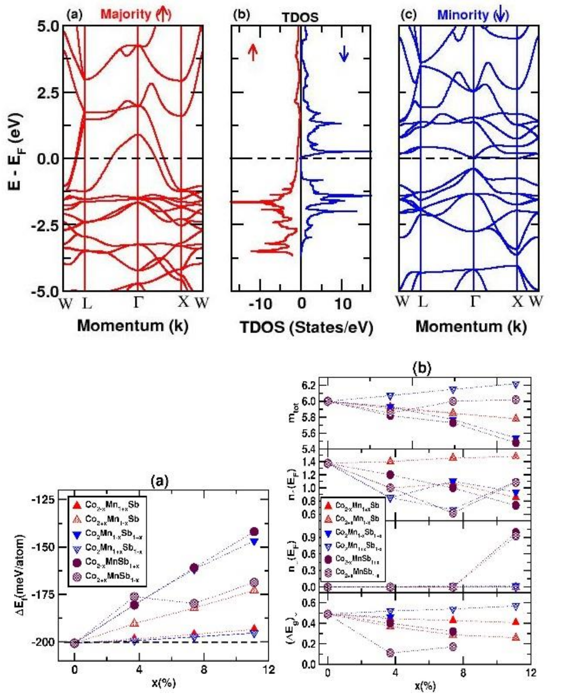


*Figure 3. Electronic structure of the $Co_2MnSb$ alloy (left) and effect of binary antisite disorder on the formation energy ($\Delta E_F$), DOS ($n(E_F)$), bandgap ($(\Delta E_g)\downarrow$), and total magnetic moment ($m_t$) (right).*

## Research Project 3

Transport properties of III-V semiconductors

In this research project, the goal was to investigate the transport properties of strained (along various directions) GaAs/InAs and In/Ga-doped GaAs/InAs by using a theoretical tool (BoltzTrap code). We discovered a significant enhancement in the electrical conductivity of strained GaAs/InAs (Figure 4). Increasing the electrical conductivity consequently enhanced the figure of merit. Transport properties of GaAs/InAs under various doping concentrations are being studied.

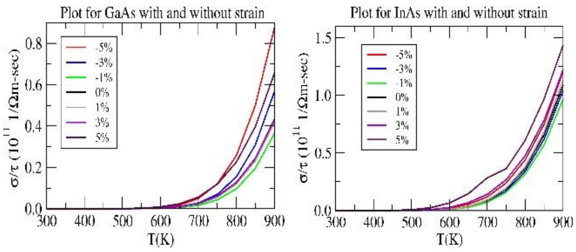


*Figure 4. Plot of the electrical conductivity versus the temperature (T) under various strained conditions*

## Research Project 4

Effect of transition metal doping on the magnetocrystalline anisotropy energy (MAE) of Fe2P

This project is in collaboration with our colleague, Dr. Soumya Bhat (IKST). The goal is to reduce the MAE of $Fe_2P$ and enhance its Curie temperature ($T_C$) through transition metal doping. We found that at specific doping concentrations of transition metals, the MAE decreased and $T_C$ increased significantly.

## References

1. G.D. Mahan, J.O. Sofo, Proc. Natl. Acad. Sci. Unit. States Am. 93 (1996) 7436.
2. C. Felser, G. H. Fecher, and B. Balke, Angew. Chem., Int. Ed. 46, 668 (2007).
3. *"Half-Metallic Alloys"*, edited by I. Galanakis and P. H. Dederichs (Springer, Berlin, 2005).
4. T. Graf, C. Felser, S.S.P. Parkin, Prog. Solid State Chem. 39 (2011) 1 (references therein).
5. Enamullah and Seung-Cheol Lee, J. Alloys Comp. 742, 903-909 (2018).
6. Enamullah and Seung-Cheol Lee, under review in J. Appl. Phys.
7. A. Rajanikanth, Y. K. Takahashi, and K. Hono, J. Appl. Phys. 101, 023901 (2007).
8. S. Picozzi and A. Continenza and A. J. Freeman, Phys. Rev. B 69, 094423 (2004).

# First-Principles Investigation of the Structural and Magnetic Properties of $Fe_2P$

**Soumya Bhat**
Post Doctoral Fellow

**Soumya.bhat@@ikst.res.in**

## Introduction

$Fe_2P$ has tremendous technological importance because it demonstrates unique magnetic properties, such as large uniaxial MAE [1], magnetocaloric properties [2], and magnetoelastic properties [3], due to which it has wide industrial applications. In recent years, $Fe_2P$ has also been identified as a potential electrocatalyst for hydrogen evolution reactions [4]. In addition to its industrial significance, $Fe_2P$ is also interesting to geophysicists because $Fe_2P$ is a major component of meteorites in the form of barringerite and allabogdanite [5].

At ambient conditions, $Fe_2P$ crystallizes in the hexagonal C22-type structure with a space group $P\overline{6}2m$ [6]. The unit cell of the hexagonal C22 phase is composed of three formula units with three Fe atoms occupying 3*f* sites ($Fe_I$), three Fe atoms in 3*g* sites ($Fe_{II}$), two P atoms occupying 2*c* sites ($P_I$), and one P atom in the 1*b* site ($P_{II}$). The $Fe_I$ atom is surrounded by four P atoms, whereas the $Fe_{II}$ atom is surrounded by five P atoms, which are referred to as tetrahedral and pyramidal sites, respectively. The structure can be expressed as Fe3 triangles in the *ab* plane, with P occupying the alternate layers. High pressure and high temperature X-ray diffraction experiments on $Fe_2P$ [7, 8] disclosed structural phase transition from C22 to the orthorhombic C23 structure with space group *Pnma* under compression. The unit cell of orthorhombic C23 structure has four formula units and shares a similar pseudo-hexagonal arrangement of iron atoms as in the C22 structure. However, the arrangement of P atoms is different from that of the hexagonal structure in that half of the P(II) atoms are neighboring empty Fe3 triangles along the *c*-direction. In contrast to the experimental observation, the first-principles calculations based on the DFT predicted the C23 structure as the stable phase of $Fe_2P$ [9]. The discrepancy in the experimental observation and theoretical prediction of the ground state structure of $Fe_2P$ makes it essential to carry out a systematic analysis.

To fill in the gap between the theory and experiment, we investigated the ground state structural stability of $Fe_2P$ using first-principles calculations based on the DFT. Furthermore, we explored the effect of alloying transition metal elements on the structure and magnetic properties of $Fe_2P$. We are also working in collaboration with a research group at IIT BHU on the low-temperature structural and magnetic properties of $Fe_2P$.

## Role of Zero-Point Effects in Stabilizing the Ground State Structure of Bulk $Fe_2P$

To examine the stability of $Fe_2P$ under hydrostatic pressure, the total energy as a function of volume for both the phases of $Fe_2P$ was determined. The results are displayed in Figure 1. The enthalpy of the C23 phase was calculated in reference to the C22 phase as a function of the hydrostatic pressure (inset of Figure 1). Calculations indicate that the C23 phase has lower energy (−10.4 meV/atom) than the C22 phase under the calculation conditions of absolute temperature and pressure. To validate the generalized gradient approximation (GGA) functional used in our DFT calculations, we performed calculations using local density approximation (LDA). Furthermore, calculations were carried out with on-site Hubbard corrections as well as van der Waals interactions for both the GGA and LDA. All these calculations confirmed our results obtained using the GGA. The results predicted the C23 phase as the ground state structure of $Fe_2P$, and therefore, contradicted the experimental observation. A possible reason for the above discrepancy between the experiments and theoretrical results could be the zero-point vibrational energy contribution. However, the calculated zero-point vibrational energy difference (4.6 meV/atom) favors the C22 phase but is not large enough to stabilize the C22 phase.

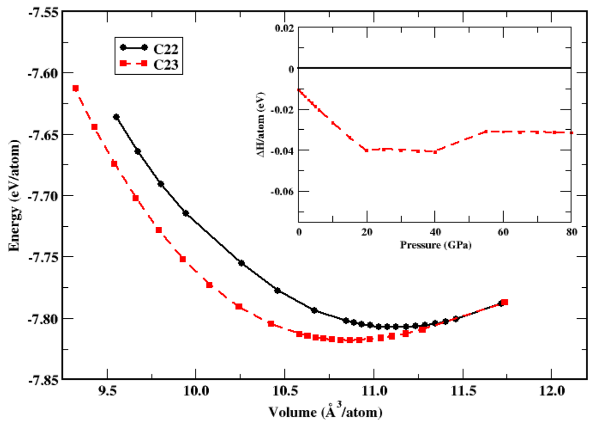

*Figure 1. Variation of energy as a function of volume for the C22 and C23 phases of $Fe_2P$. Inset: Calculated enthalpy of the C23 phase with reference to the C22 phase as a function of pressure.*

In Fe-pnictide systems, spin fluctuations are very important. To explore whether the C22 phase could possibly be stabilized by zero-point spin fluctuation (ZPSF), we write the total energy of the system as $E = E_{\mathrm{DFT}} + E_{\mathrm{ZPV}} + E_{\mathrm{ZPSF}}$ where $E_{\mathrm{DFT}}$ is the electronic energy obtained from DFT calculation, $E_{\mathrm{ZPV}}$ is the energy correction due to zero-point vibration, and $E_{\mathrm{ZPSF}}$ is the ZPSF energy. We estimated $E_{\mathrm{ZPSF}}$ from the magnetic susceptibility calculations and the ZPSF energy difference was calculated to be 23.6 meV/atom. Accordingly, we can conclude that the ZPSF energy difference is large enough to overcome the DFT-predicted energy difference (i.e., −10.4 meV/atom) and hence stabilizes the C22 phase. Thus, our results indicate that to obtain the correct ground state structure of $Fe_2P$ from the first-principles based methods, considering zero-point effects, such as the zero-point vibrations and spin fluctuations, is necessary. This presents a unique result where quantum effects significantly influence the structural stability of a bulk material [10].

## Effects of Alloying on the Magnetocrystalline Anisotropy of $Fe_2P$

The MAE is an essential property of hard magnetic materials that are widely utilized as permanent magnets and perpendicularly magnetized films. Because spin-orbit interactions have a relativistic effect on electron motion, a large magnetocrystalline anisotropy has been observed from compounds with heavy elements, such as rare-metal and rare-earth elements [11]. However, from an application point of view, there has been a strong demand for rare-element-free magnets. Among these materials, iron phosphide ($Fe_2P$) stands out as a particularly interesting material due its known large MAE and sufficiently large saturation moment. Moreover, $Fe_2P$ is composed of cheap and widely available elements. However, due to its low Curie temperature, ($T_C$) of 216 K [12], $Fe_2P$ is impractical for room temperature applications. Earlier studies have exhibited considerable enhancement in $T_C$ by alloying $Fe_2P$ with Ni, Co, Si, and B [12–16], which making it suitable for room temperature applications. We examined the effect of Co, Ni, Cu, and Zn substitution on the structural and magnetic properties of $Fe_2P$ by using first-principles calculations.

For our calculations, one out of six Fe atoms, either from the $Fe_I$ site or $Fe_{II}$ site was substituted with a transition metal, which resulted in the formula $(Fe_{1-x}M_x)_2P$, with x = 0.16 and M = Co, Ni, Cu, and Zn. Through the comparison of the total energies, we analyzed the preferential occupation by these elements of two inequivalent Fe sites of $Fe_2P$. Our calculations indicated that Co and Ni substituted Fe preferentially at the tetrahedral site, whereas Cu and Zn substituted Fe at the pyramidal site.

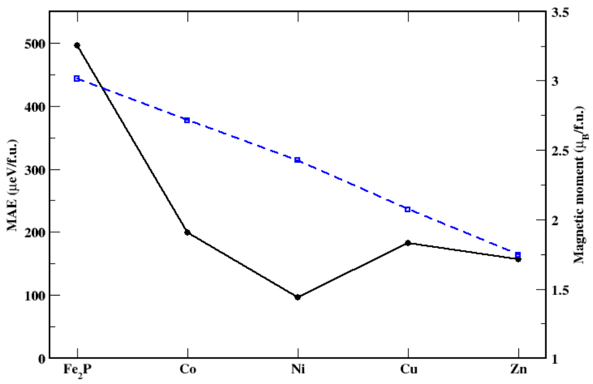


*Figure 2. Calculated MAE and magnetic moment for $Fe_2P$, and Co-, Ni-, Cu-, and Zn-substituted $Fe_2P$*

For all the studied alloys, the total magnetic moment was less than that of $Fe_2P$ and decreased linearly from Co to Zn substitution (Figure 2). The computed MAE for $Fe_2P$ was 496 μeV/fu, with the magnetic easy axis oriented along the [001] direction, which is in excellent agreement with the experimental result [13]. For all M substitutions, the calculated MAE was lower than that of $Fe_2P$. Similar to pristine $Fe_2P$, Co-, Cu-, and Zn-substituted $Fe_2P$ also had [001] as the magnetization easy axis. For Ni substitution, the magnetic easy axis was along the [100] direction, with the lowest MAE (97 μeV/fu) among all the alloys under consideration (Figure 2). The decrease in the MAE was substantial (approximately 80%) for a small substitution of Ni, whereas the decrease in the magnetic moment was marginal (approximately 20%). Therefore, $(Fe_{1-x}Ni_x)_2P$ compounds can be useful for high-temperature applications, in which high magnetization and low MAE are the design requirements.

## Conclusions and Outlook

Typically, zero-point effects are crucial for the stability of layered or 2D materials, such as boron nitride [17]. However, our calculations disclosed a rare case where quantum effects played a pivotal role in the structural stability of a 3D material. According to our calculations, we can predict the possibility of magnetic-field-induced structural quantum phase transition in $Fe_2P$. Experimental verification and deep theoretical understanding of the predicted quantum phase transition can be envisioned as the future scope of this research. In the case of $Fe_2P$-based alloys, because Co-, Cu-, and Zn-substituted $Fe_2P$ have their magnetic easy axis oriented along the [001] direction and $T_C$ above room temperature, they can be used in perpendicular magnetic recording applications. As the MAE of $Fe_2P$-

based alloys is quite promising, we are now working on obtaining a particular doping concentration that provides the lowest MAE in combination with a high $T_C$ and large magnetic moment.

## References

1. L. Caron, M. Hudl, V. Höglin, N. H. Dung, C. P. Gomez, M. Sahlberg, E. Brück, Y. Andersson, and P. Nordblad, Phys. Rev. B **88**, 94440 (2013).
2. M. Fries, L. Pfeuffer, E. Bruder, T. Gottschall, S. Ener, L. V. B. Diop, T. Gröb, K. P. Skokov, and O. Gutfleisch, Acta Mater. **132**, 222 (2017).
3. Z. Gercsi, E. K. Delczeg-Czirjak, L. Vitos, A. S. Wills, A. Daoud-Aladine, and K. G. Sandeman, Phys. Rev. B **88**, 24417 (2013).
4. H. Y. Zhao, D. Li, P. Bui, and S. T. Oyama, Appl. Catal. A Gen. **391**, 305 (2011).
5. S. N. Britvin, N. S. Rudashevsky, S. V Krivovichev, P. C. Burns, and Y. S. Polekhovsky, Am. Mineral. **87**, 1245 (2002).2
6. B. Carlsson, M. Gölin, and S. Rundqvist, J. Solid State Chem. **8**, 57 (1973).
7. P. Dera, B. Lavina, L. A. Borkowski, V. B. Prakapenka, S. R. Sutton, M. L. Rivers, R. T. Downs, N. Z. Boctor, and C. T. Prewitt, Geophys. Res. Lett. **35**, (2008).
8. T. Gu, X. Wu, S. Qin, C. McCammon, and L. Dubrovinsky, Eur. Phys. J. B **86**, 311 (2013).
9. X. Wu and S. Qin, in *J. Phys. Conf. Ser.* (IOP Publishing, 2010), p. 12110.
10. Y. Kota and A. Sakuma, J. Phys. Soc. Japan **83**, 34715 (2014).
11. Soumya S. Bhat, Kapil Gupta, Satadeep Bhattacharjee and Seung Cheol Lee, under review in J. Phys. Condens. Matter.
12. R. Fruchart, A. Roger, and J. P. Senateur, J. Appl. Phys. **40**, 1250 (1969).
13. O. Beckman and L. Lundgren, Handb. Magn. Mater. **6**, 181 (1991).
14. R. Chandra, S. Bjarman, T. Ericsson, L. Häggström, C. Wilkinson, R. Wäppling, Y. Andersson, and S. Rundqvist, J. Solid State Chem. **34**, 389 (1980).
15. A. Catalano, R. J. Arnott, and A. Wold, J. Solid State Chem. **7**, 262 (1973).
16. P. Jernberg, A. A. Yousif, L. Häggström, and Y. Andersson, J. Solid State Chem. **53**, 313 (1984).
17. K. Albe, Phys. Rev. B **55**, 6203 (1997)

# Structural Materials/III-V Semiconductors/ Catalytic Materials

**P. Iyyappa Rajan**

Post Doctoral Fellow

**iyyappa.rajan@ikst.res.in**

## Research Project 1: Structural Materials

(This project is supervised by Dr. Seung-Cheol Lee and Dr. Mahesh Chandran.)

Global demands focusing on increasing energy efficiency and reducing $CO_2$ emissions in steam power plants has resulted in high operating temperatures and pressures in power plants. Consequently, in the past decades, enormous attention was given to the design and development of advanced materials that exhibited high creep rupture strength, resistance toward oxidation, excellent thermal fatigue properties, and cost-effectiveness. Chromium (Cr) (9–12 wt%) martensitic heat-resistant steels are commonly known for their extensive applications in turbines, steam-line pipes, and boilers for steam power plants. However, the practical applicability of these types of steels is limited at high temperature ranges, where they are exposed for a long time due to the dramatic breakdown of their creep rupture strength. The root cause of the degradation in creep rupture strength is due to the formation of large, fine, and coarse precipitate known as the Z-phase. The formula of the Z-phase precipitate was observed to be that of a complex nitride Cr(Nb,V)N and did not contribute significantly in precipitate strengthening, thereby reducing the creep rupture strength.

Z-phase formation and stability in heat-resistant steels is crucial for increasing the energy efficiency of steel technology. In the experiment, we investigated the formation mechanism and stability of the Z-phase Cr(Nb,V)N based on the first-principles DFT calculations and validated our results with the reported experimental observations. Finally, according to our calculated results, we proposed a hypothesis for the formation and stability of the Z-phase. This hypothesis can provide an excellent guide to researchers for controlling the formation of the Z-phase. Figures 1.1 and 1.2 depict the mixing enthalpy behavior of two Z-phases (CrNbN and CrVN) and their formation mechanism from the precipitates ($Cr_2N$, NbC, and NbN) in the martensitic heat-resistant steels.

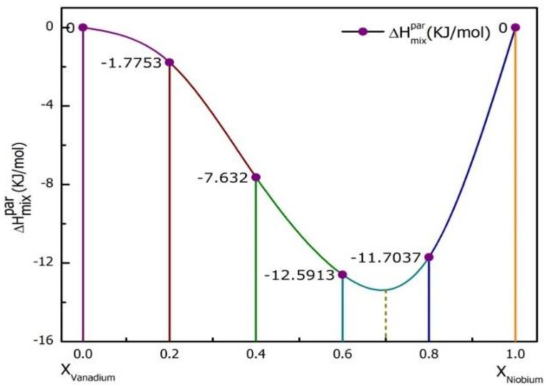


*Figure 1.1 The solid solution mixing enthalpy for Cr(Nb,V)N calculated using the parametric approach*

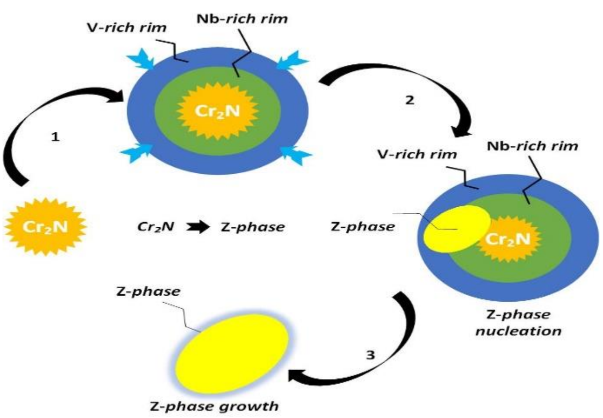


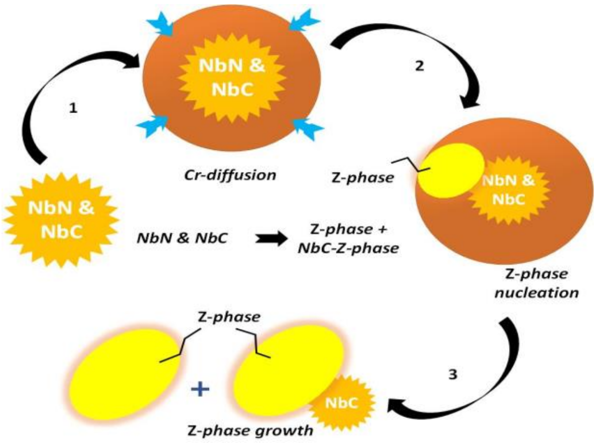


*Figure 1.2 Z-phase formations from $Cr_2N$, NbC, and NbN precipitates in the martensitic heat-resistant steel*

## Research Project 2: III-V Semiconductors

(This project is supervised by Dr. Seung-Cheol Lee and Dr. Satadeep Bhattacharjee)

III-V semiconductors are known for their vital applications in modern electronic devices. In particular, the growth along nonpolar (110) surfaces of GaAs and InAs are given more importance in the thin-film process technology. In general, the thin-film growth of GaAs/InAs-segregated semiconductors is strongly influenced by the surface energy and segregation behavior. The understanding of these parameters in experiments is quite difficult. Therefore, we utilized the first-principles DFT method to understand the segregation behavior of Ga atoms in the InAs surface and bulk regions as well as the segregation behavior of In atoms in the GaAs surface and bulk regions. Some of the key findings of this project are as follows:

1) The surface energy of the InAs surface is lower than that of the GaAs surface.
2) In atoms tend to segregate more easily in the GaAs surface than the bulk. The trend reverses in the case of Ga segregation in the InAs surface slab, where Ga atoms segregate favorably in the bulk regions of InAs although Ga segregation in the second layer (subsurface) is feasible.
3) The segregation behavior was calculated on the basis of 25–100 atom% of doping per layer. The strain plays a significant role in the energetics of Ga/InAs and In/GaAs.

In Figures 2.1 and 2.4, the segregation energy trend of (i) Ga in the InAs (110) surface and bulk and (ii) In in the GaAs (110) surface and bulk is displayed along with the effect of strain.

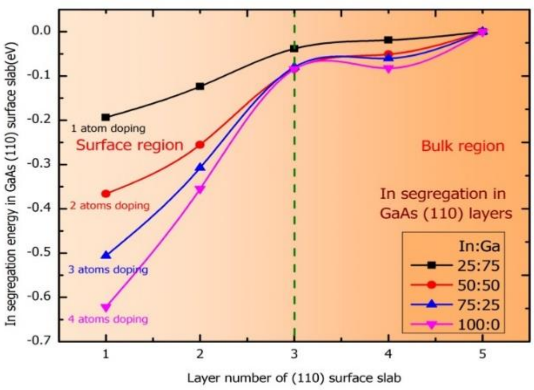


*Figure 2.1*

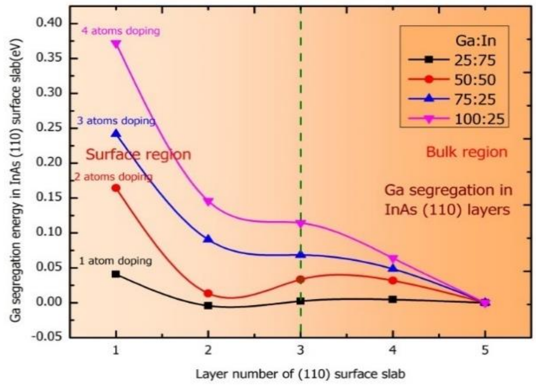


*Figure 2.2*

*Figures 2.1 and 2.2: Effect of Ga/In doping on the GaAs and InAs (110) surfaces and bulk regions at various doping concentrations*

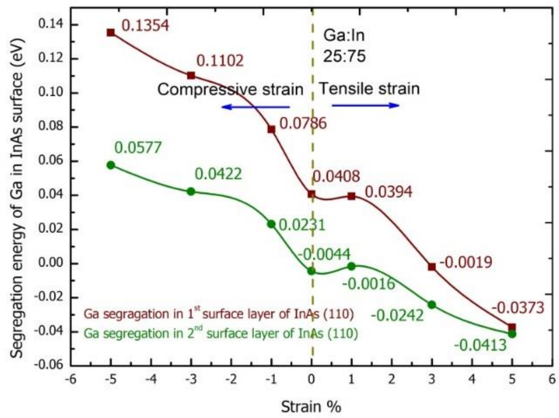


*Figure 2.3*

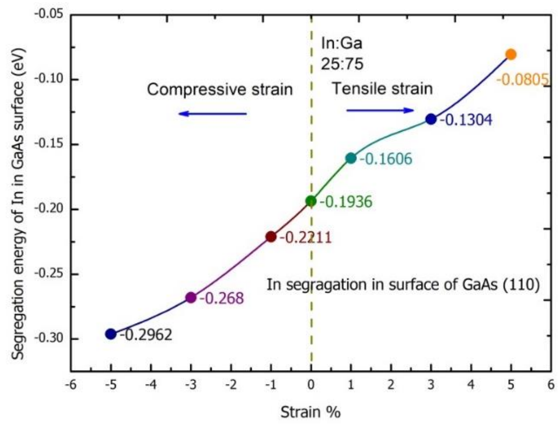


*Figure 2.4*

*Figures 2.3 and 2.4: Effect of strain on Ga/In doped in the GaAs/InAs (110) surfaces*

## Research Project 3: Catalytic Materials

(This project is supervised by Dr. Seung-Cheol Lee and Dr. Satadeep Bhattacharjee)

We are also involved in the design and development of new catalysts for environmental remediation, particularly focusing on new or modified transition-metal-based compounds. One such project involves the investigation of the catalytic activity of transition metal sulfides (MS) toward the degradation of phenol in the presence of the primary oxidant ($H_2O_2$) through the adsorption–desorption mechanism. This project involved an experimental collaboration with our research colleagues from South Korea. We performed the supportive calculations to validate the obtained experimental results. The adsorption energies, ($E_{ads}$) of the $H_2O_2$ and OH molecules over the MS surface were calculated for the hexagonal (0001) surfaces of MS with metal termination. Both the experimental results and DFT-simulated results agreed with each other. The pictorial representation of the MS surface slabs obtained using the adsorption energies ($E_{ads}$) and the experimental rate of the phenol consumption reaction with MS catalysts are illustrated in Figures 3.1 and 3.3, respectively.

Furthermore, we also investigated the role of magnetism in the catalytic activity of transition metals, such as Fe, Co, Ni, NiPt, and FePt, by using the improved d-band center model. The spin-polarized DFT calculations were employed and the adsorption energies of molecules such as $N_2$, $F_2$, $H_2$, $O_2$, and NO over the active sites of the transition metal surfaces were calculated. The post-processing calculations were carried out with the improved d-band center model, as proposed in the previously published research paper [1] of our scientists in the IKST.

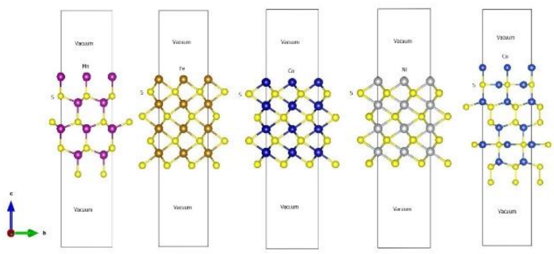


*Figure 3.1 The MS surface slabs (where M = Mn, Fe, Co, Ni, and Cu) used for the DFT calculations*

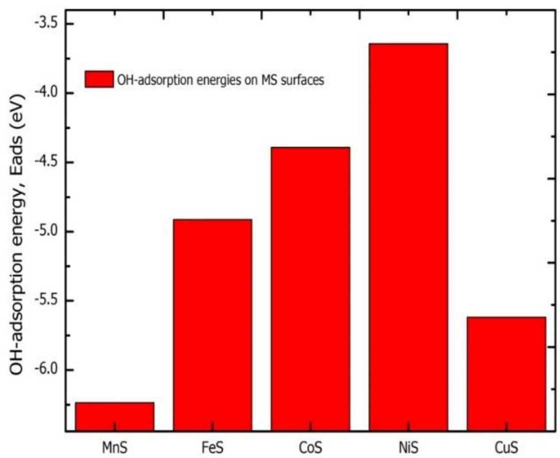

*Figure 3.2 Plot of the MS-OH (where M = Mn, Fe, Co, Ni, and Cu) adsorption energies ($E_{ads}$) (DFT calculations result)*

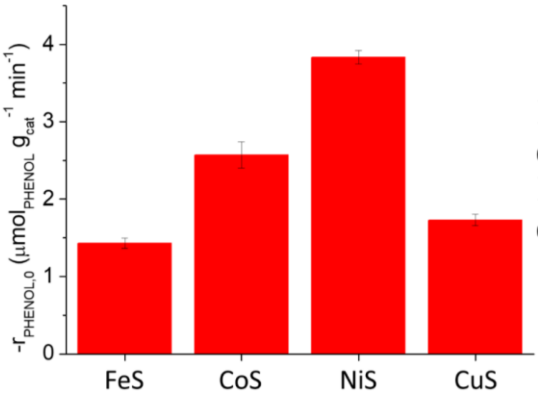


*Figure 3.3 Rate of the phenol consumption reaction with MS catalysts (experimental result)*

## Reference

1. An improved d-band model of the catalytic activity of magnetic transition metal surfaces, **Satadeep Bhattacharjee**, Umesh V. Waghmare and **Seung-Cheol Lee**, **Sci. Rep**., 6, 35916. 10.1038/srep 35916

# Machine Learning/Video Analytics

**Renuka Patnaik**

Data Analytics Specialist

**renuka.patnaik@ikst.res.in**

## Predicting the Occurrence of Essential Hypertension Using Annual Health Records

A machine learning library was developed to predict the occurrence of essential hypertension (whose international disease code is I10) using repeated annual health examination data.

### Dataset Description

For our study, we used data from the Korean National Health Insurance Corporation, which contains the electronic medical records of patients having their annual general health check-ups between 2002 and 2013 (12 years). The I10 group consists of data from patients who have no prior history of I10 for 10 consecutive years and were subsequently diagnosed with it in the 11th year. The control group consisted of patients with some disease other than I10 in 11th year. This labeled data that consisted of 4707 patients (3994 males and 713 females) formed the I10 group and was used for training our models. The number of patients in the control group was maintained the same as that in the I10 group.

### Factors of Interest

Based on the preliminary analysis of data, we used the major risk factors, demographics, and income-quantile details in our study. Some of them are described in the following text.

*i.* **Health check-up data:** Among several variables from the dataset, some exhibited a significant association with hypertension, including the systolic and diastolic blood pressure values (SBP and DBP, respectively), body mass index (BMI), and family history.

*ii*. **Demographic details:** Demographic details, such as age and geographic location, were considered as input variables.

*iii.* **Income-quantile details:** People in the high income-quantile group (approximately 44%) were at a higher risk of I10 compared with other income-quantile groups. Such a correlation implied the requirement of an economic indicator in the model. As a result, the income-quantile was made a variable in our study.

**Methodology**

The supervised classifiers considered for prediction were naïve bayes, support vector machines, multilayer perceptron, random forest, and logistic regression.

**Results**

The performance measures for various classification models are provided in Table I. The accuracy is in the range of 66%–81% when considering the past 2–10 years. No significant change was observed in the performance of different models. The results of SVM are described accurately in detail in the following text.

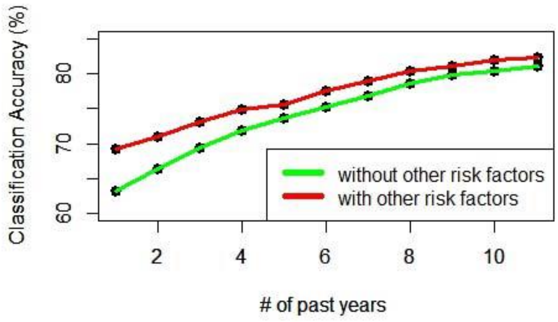


*Figure 1: Comparison of classification accuracies using SVM according to the number of past years with and without other risk factors, such as BMI, DBP, total cholesterol, and family history*

Figure 1 displays the classification accuracy using SVM when the health records regarding the number of years were included in the model. Risk factors such as BMI, DBP, total cholesterol, and family history increased the accuracy of the model when only data from a few years was included. To improve the classification accuracy, the risk factors were considered for the past two years, along with other input variables, and the accuracies were plotted for I10, as illustrated in Figure 2a. By including data regarding risk factors from the past 2 years, the accuracy improved. No significant improvement was observed in the performance beyond two years. The ROC curves obtained by considering past two years' data of risk factors for different SVM models ($C_i$, $i$ = 2, 3, ... 11) are depicted in Figure 2b. The area under the ROC curve (0.8977) remained constant after 10 years (Table. II). Therefore, it required 10 years of data to accurately predict the onset of I10. The accuracy improved from 71.28% to 80.23% (Table. I) when past personal medical history from 2–11 years was considered for the SVM.

TABLE I: Comparison of the performance of models for test set (Essential Hypertension)

| # of past years | Method | $\kappa$-score | Sensitivity (Recall) | Specificity | Precision | Accuracy | F1-score | # of hidden nodes |
|---|---|---|---|---|---|---|---|---|
| 2 | NB | 0.3441 | 0.7884 | 0.5551 | 0.6424 | 0.6718 | 0.7079 | - |
| 3 | NB | 0.3589 | 0.7715 | 0.5870 | 0.6544 | 0.6792 | 0.7081 | - |
| 4 | NB | 0.3834 | 0.7703 | 0.6127 | 0.6684 | 0.6915 | 0.7157 | - |
| 5 | NB | 0.4177 | 0.7606 | 0.6569 | 0.6920 | 0.7087 | 0.7247 | - |
| 6 | NB | 0.4385 | 0.7666 | 0.6716 | 0.7029 | 0.7191 | 0.7334 | - |
| 7 | NB | 0.4763 | 0.7690 | 0.7071 | 0.7269 | 0.7381 | 0.7474 | - |
| 8 | NB | 0.5153 | 0.7908 | 0.7243 | 0.7440 | 0.7575 | 0.7667 | - |
| 9 | NB | 0.5239 | 0.7872 | 0.7365 | 0.7517 | 0.7619 | 0.7690 | - |
| 10 | NB | 0.5422 | 0.7896 | 0.7525 | 0.7637 | 0.7710 | 0.7765 | - |
| 11 | NB | 0.5543 | 0.7969 | 0.7574 | 0.7690 | 0.7771 | 0.7827 | - |
| 2 | SVM | 0.4256 | 0.6941 | 0.7316 | 0.7238 | 0.7128 | 0.7086 | - |
| 3 | SVM | 0.4439 | 0.6965 | 0.7475 | 0.7366 | 0.7220 | 0.7160 | - |
| 4 | SVM | 0.4597 | 0.7001 | 0.7598 | 0.7471 | 0.7300 | 0.7228 | - |
| 5 | SVM | 0.4768 | 0.7050 | 0.7721 | 0.7581 | 0.7385 | 0.7306 | - |
| 6 | SVM | 0.5254 | 0.7388 | 0.7868 | 0.7783 | 0.7628 | 0.7581 | - |
| 7 | SVM | 0.5290 | 0.7473 | 0.7819 | 0.7764 | 0.7646 | 0.7616 | - |
| 8 | SVM | 0.5668 | 0.7618 | 0.8051 | 0.7985 | 0.7835 | 0.7797 | - |
| 9 | SVM | 0.5753 | 0.7690 | 0.8064 | 0.8010 | 0.7877 | 0.7847 | - |
| 10 | SVM | 0.5959 | 0.7836 | 0.8125 | 0.8090 | 0.7980 | 0.7961 | - |
| 11 | SVM | **0.6045** | 0.7872 | 0.8174 | 0.8138 | **0.8023** | **0.8002** | - |
| 2 | LR | 0.4303 | 0.7158 | 0.7145 | 0.7176 | 0.7152 | 0.7167 | - |
| 3 | LR | 0.4242 | 0.7158 | 0.7083 | 0.7133 | 0.7121 | 0.7145 | - |
| 4 | LR | 0.4498 | 0.7267 | 0.7230 | 0.7267 | 0.7249 | 0.7267 | - |
| 5 | LR | 0.4547 | 0.7158 | 0.7390 | 0.7354 | 0.7274 | 0.7255 | - |
| 6 | LR | 0.5009 | 0.7461 | 0.7549 | 0.7552 | 0.7505 | 0.7506 | - |
| 7 | LR | 0.5033 | 0.7533 | 0.7500 | 0.7533 | 0.7517 | 0.7533 | - |
| 8 | LR | 0.5471 | 0.7751 | 0.7721 | 0.7751 | 0.7736 | 0.7751 | - |
| 9 | LR | 0.5824 | 0.7993 | 0.7831 | 0.7888 | 0.7912 | 0.7940 | - |
| 10 | LR | 0.5715 | 0.7908 | 0.7806 | 0.7851 | 0.7857 | 0.7880 | - |
| 11 | LR | 0.5909 | **0.8017** | 0.7892 | 0.7940 | 0.7955 | 0.7978 | - |
| 2 | RF | 0.4065 | 0.6409 | 0.7659 | 0.7351 | 0.7034 | 0.6848 | - |
| 3 | RF | 0.4454 | 0.6626 | 0.7831 | 0.7559 | 0.7229 | 0.7062 | - |
| 4 | RF | 0.4392 | 0.6626 | 0.7770 | 0.7507 | 0.7198 | 0.7039 | - |
| 5 | RF | 0.4880 | 0.6796 | 0.8088 | 0.7827 | 0.7442 | 0.7275 | - |
| 6 | RF | 0.5256 | 0.7037 | 0.8223 | 0.8006 | 0.7630 | 0.7490 | - |
| 7 | RF | 0.5353 | 0.7146 | 0.8211 | 0.8019 | 0.7679 | 0.7558 | - |
| 8 | RF | 0.5560 | 0.7183 | 0.8382 | 0.8182 | 0.7782 | 0.7650 | - |
| 9 | RF | 0.5694 | 0.7328 | 0.8370 | 0.8200 | 0.7849 | 0.7739 | - |
| 10 | RF | 0.5876 | 0.7497 | 0.8382 | 0.8245 | 0.7940 | 0.7853 | - |
| 11 | RF | 0.5912 | 0.7545 | **0.8370** | **0.8243** | 0.7958 | 0.7879 | - |
| 2 | MLP | 0.3216 | 0.5659 | 0.7561 | 0.7016 | 0.6610 | 0.6265 | (11) |
| 3 | MLP | 0.3942 | 0.6445 | 0.7500 | 0.7232 | 0.6972 | 0.6816 | (11) |
| 4 | MLP | 0.4029 | 0.6239 | 0.7794 | 0.7414 | 0.7017 | 0.6776 | (12) |
| 5 | MLP | 0.4258 | 0.6626 | 0.7635 | 0.7395 | 0.7131 | 0.6990 | (13) |
| 6 | MLP | 0.4575 | 0.6663 | 0.7917 | 0.7642 | 0.7290 | 0.7119 | (13) |
| 7 | MLP | 0.4439 | 0.6929 | 0.7512 | 0.7384 | 0.7220 | 0.7149 | (14) |
| 8 | MLP | 0.4792 | 0.7086 | 0.7708 | 0.7581 | 0.7397 | 0.7325 | (15) |
| 9 | MLP | 0.4912 | 0.7376 | 0.7537 | 0.7522 | 0.7456 | 0.7448 | (15) |
| 10 | MLP | 0.4974 | 0.7267 | 0.7708 | 0.7627 | 0.7488 | 0.7443 | (16) |
| 11 | MLP | 0.4767 | 0.7122 | 0.7647 | 0.7542 | 0.7385 | 0.7326 | (17) |

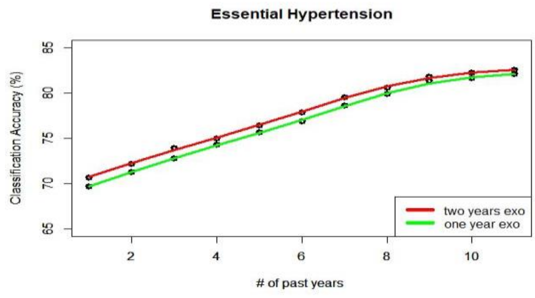


*(a)*

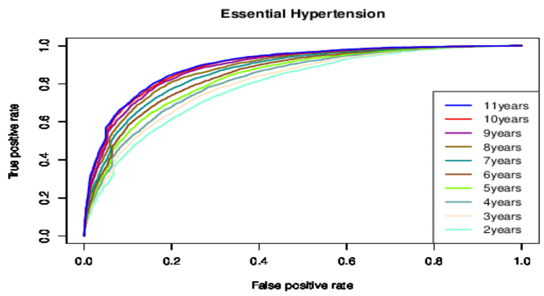


*(b)*

*Figure 2: Performance evaluation of essential hypertension (I10) by using the SVM*

TABLE II: AUROC

| # of past years | I10 |
|---|---|
| 2 | 0.8051 |
| 3 | 0.8192 |
| 4 | 0.8341 |
| 5 | 0.8456 |
| 6 | 0.8599 |
| 7 | 0.8713 |
| 8 | 0.8824 |
| 9 | 0.8922 |
| 10 | 0.8977 |
| 11 | 0.9004 |

## Video Synopsis

Millions of surveillance cameras operate 24 × 7 and generate huge amounts of visual data for processing. However, the retrieval of important activities from such large data can be time consuming. Therefore, researchers are working on finding solutions to present hours of visual data in a compressed but meaningful manner. Video synopsis is one of the techniques to represent activities using relatively short-duration clips. So far, two main approaches have been used by researchers to address this problem, namely, synopsis by tracking moving objects and synopsis by clustering moving objects. Synopses outputs mainly depend on the tracking, segmenting, and shifting of moving objects temporally as well as spatially. In many situations, tracking fails. Thus, multiple trajectories of the same object are produced. Due to this, the object may appear and disappear multiple times within the same synopsis output, which is misleading. This also leads to discontinuity and often can be confusing to the viewer of the synopsis. In this project, a new approach was proposed for generating compressed video synopsis by grouping tracklets of moving objects. Grouping helps to generate a synopsis where chronologically related objects appear together with meaningful spatio-temporal relation. This proposed method produced continuous but clear synopses when tested on publicly available video datasets as well as in-house video datasets.

This project was carried out in collaboration with Dr. Debi Prosad Dogra, Assistant Professor, School of Electrical Sciences, IIT Bhubaneswar.

## References

1. Renuka Patnaik, Mahesh Chandran, Seung-Cheol Lee, Anurag Gupta, Chansoo Kim, Changsoo Kim, "*Predicting the occurrence of essential hypertension using annual health records*", **IEEE International Conference on Advances in Electronics, Computers and Communications** (ICAECC), 2018
2. Ahmed, D. P. Dogra, S. Kar, R. Patnaik, H. Choi, I. Kim, S.C. Lee, '*Video Synopsis Generation Using Spatio-Temporal Groups*', **IEEE International Conference on Signal and Image Processing Applications** (ICSIPA), 2017

# Publications

Authors: J. Fransson, D. Thonig, P. F. Bessarab, S. Bhattacharjee, J. Hellsvik, and L. Nordström
*Microscopic theory for coupled atomistic magnetization and lattice dynamics*, PHYSICAL REVIEW MATERIALS 1, 074404-1, 074404-20(2017)

Authors: Swastika Banerjee, Jaehong Park, Cheol Seong Hwang, Jung-Hae Choi, Seung-Cheol Lee, and Swapan K. Pati
*Regulation of transport properties by polytypism: a computational study on bilayer MoS2*, Physical chemistry chemical physics: PCCP, 2017, 19, 21285-21286 (2017)

Authors: Nam-In Kim, Rana Arslan Afzal, Sung Ryul Choi, Sung Won Lee, Docheon Ahn, Satadeep Bhattacharjee, Seung-Cheol Lee, Jung Hyun Kim and Jun-Young Park
*Highly active and durable nitrogen doped-reduced graphene oxide/double perovskite bifunctional hybrid catalysts*, Journal of Materials Chemistry A, 25, 13019-13031 (2017)

Authors: Seok Ki Kim, Jaehoon Kim, and Seung-Cheol Lee
*Surface-termination dependence of propanoic acid deoxygenation on Mo2C*, Catalysis Communications, 61-65, 99 (2017)

## Conferences

Presenter: Mahesh Chandran

*Machine Learning Configurational Energy of Multicomponent Solid Solutions — Ab Initio Calculation of Material Properties and Parameters*, 2017 Material Research Society(MRS) Fall Meeting

Presenter: Kapil Gupta

*Comprehensively Integrated Environment for Advanced Materials Simulations (CINEMAS)*, 2017 Material Research Society(MRS) Fall Meeting

Presenter: S. C. Lee

*1. Spin dependent d-ban model for the catalytic activity of magnetic transition metals*

*2. First-principles analysis of catalytic activity of phosphide surfaces*

2017 European Materials Research Society(E-MRS) Spring Meeting

Presenter: D. P. Dogra, IIT Bhubaneswar (Collaborator of Renuka Patnaik)

*Video Synopsis Generation Using Spatio-Temporal Groups*, 2017 IEEE International Conference on Signal and Image Processing Applications(IEEE ICSIPA)

# Training Programs

### January 9–February 18

**Mr. Byeong Sun Jeon**, Applied Chemistry, Hanyang University (Ansan), visited IKST to perform collaborative research on cluster expansion and the configurational stability and electrical properties of (In,Ga)As and Ga(As,Sb).

*Jan 11. Byeong Sun Jeon's presentation*

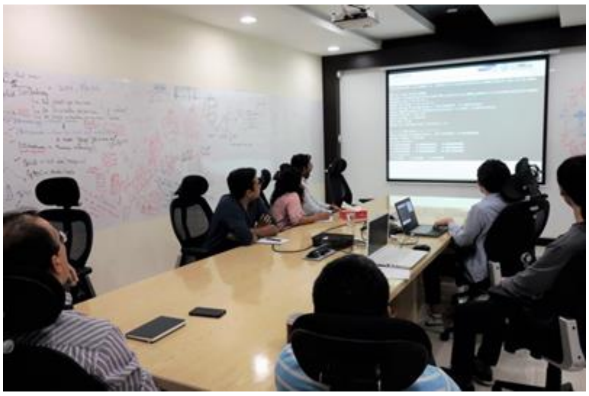

*Feb 27. Byeong Sun Jeon's result report*

### January 9–February 18

**Mr. Gyu Seung Han**, Center for Electronic Materials, KIST, visited IKST to perform collaborative research on "Cathode materials of lithium-ion battery using computational chemistry."

*Jan 11. Gyu Seung Han's presentation*

*Feb 27. Gyu Seung Han's result report*

### April 10–May 23

**Ms. Yeon Jung Lee**, EMS, Christ University, visited IKST to perform her internship on the "Medical Big Data Analysis" project under the guidance of Ms. Renuka, IKST.

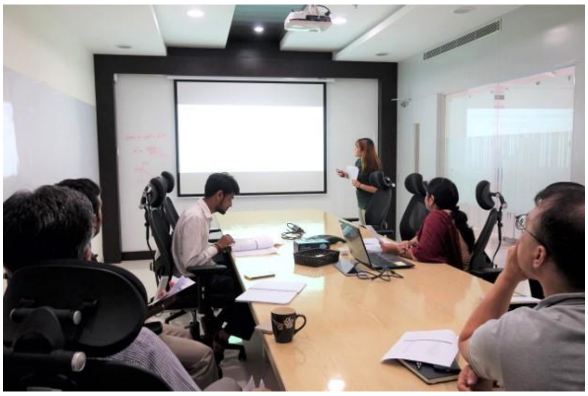

*April 20. Yeon Jung Lee's presentation*

*May 19. Yeon Jung Lee's presentation*

### May 2–July 31

**Mr. Anurag Gupta**, Dept. of Management Studies, IISc, visited IKST to perform his internship on the "Medical Big Data Analysis" project under the guidance of Ms. Renuka, IKST.

*June 1. Anurag Gupta's presentation*

*July 27. Anurag Gupta's presentation*

### May 16–July 31

**Mr. Anil Kumar**, IIT Bhubaneswar, visited IKST to perform his internship on the "Development of CINEMAS software" project under the guidance of Dr. Kapil Gupta, IKST.

## Lectures and Meetings

### January 12

**Prof. U. V. Waghmare**, Theoretical Sciences Unit, JNCASR and **Prof. Jun Hee Lee**, Dept. of Energy and Chemical Engineering, Ulsan National Institute of Science and Technology, visited IKST to attend a meeting entitled "Indo-Korea Virtual Network Center (VNC)" and conduct research collaboration on "New materials design method through materials genome."

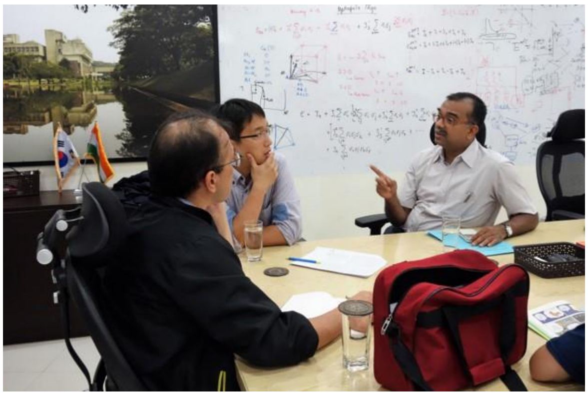

*Jan 12. Virtual Network Center(VNC) meeting*

*Jan 12. Discussion on research collaboration*

### January 31–February 3

**Prof. Sang Uck Lee**, Applied Chemistry, Hanyang University (Ansan), visited IKST to have a discussion regarding research collaboration on "Electrode stabilization technique to improve battery life" and the researcher exchange program of IKST.

*Feb 2. Prof. Sang Uck Lee's talk*

*Feb 2. Discussion on research collaboration*

### April 17

**Prof. Bhaskaran Muralidharan**, Dept. of Electrical Engineering, IIT Bombay, visited IKST to give a talk entitled “A module for linear response calculations in semiconductors using semi-classical and quantum transport formulations.”


*April 17. Prof. Bhaskaran Muralidharan’s invited talk*

### August 29–31

**Mr. Won Hyuk Choi**, International Cooperation Team, KIST, visited IKST to attend the FY 2016–17 AGM of the IKST as a proxy of shareholder, Dr. Byeong Gwon Lee, President of KIST, with Dr. Seung Cheol Lee, Ms. Malini Sridhar, and Ms. Hye Soo Lee to review the current status and activities of IKST.

*August 30. The FY 2016–17 IKST AGM was held in the conference room at the registered office*

**September 23**

Dr. Seung Cheol Lee, Director of IKST, visited the Learning Lab Bengaluru to give a guest lecture entitled "Role of IKST and employment circumstances in India" to the 2017 Seoul Digitech High School Field Learning team.


*September 23. Dr. Seung Cheol Lee's guest lecture*

**October 13**

**Prof. M. P. Gururajan**, Dept. of Metallurgical Engineering, IIT Bombay, visited IKST to give a guest lecture entitled "Phase field models for modeling microstructural evolution" and to discuss further collaborations, such as holding joint workshops and researcher exchange programs.

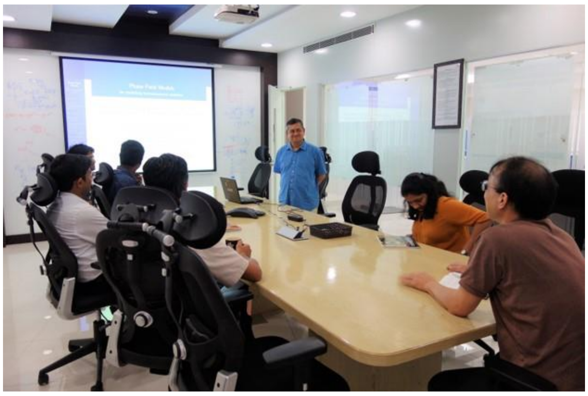
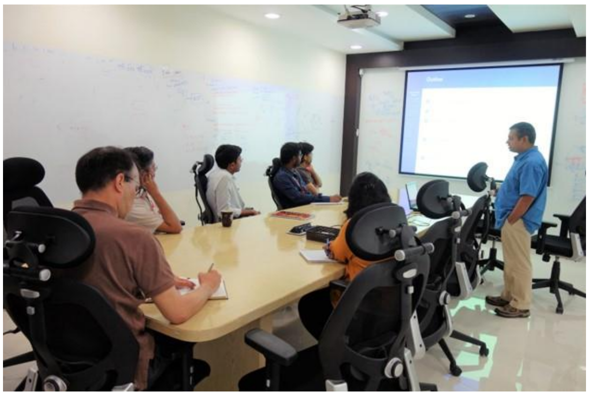

*October 10. Prof. M. P. Gururajan's guest lecture*

## December 21

**Dr. Joon Yeon Chang**, **Dr. Chong Yun Kang,** and **Mr. Sam Gyu Lee**, PSI, KIST, visited IKST to review the activities of IKST and discuss research collaborations between the PSI, KIST, and IKST.

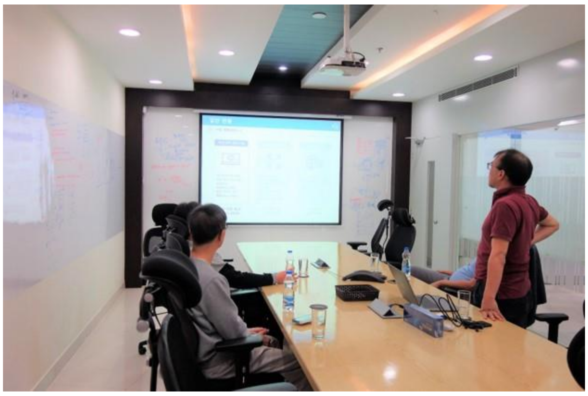

*December 21. Dr. Seung Cheol Lee's presentation introducing the performance of IKST*

# Visitors

### March 18

The **NAEK Delegation group**, including Dr. Kyung Ho Shin, KIST; Dr. Sea Hoon Lee, KIMS; Prof. Soon Hyung Hong, KAIST; Prof. Young Tai Kim, Kyung Nam University; Dr. Kwang Soo Kim, Kolon Dacc Composite; Dr. Soo Chan Lee, RIST; Dr. Sang Suk Kim, POSCO Capital; Dr. Byeong Gook Kong, Doosan Heavy Industries & Construction Com. Ltd. Corporate R&D Institute; and Ms. Eun Yeong Park (NAEK) visited IKST to explore the venue and discuss its current status.

*Jan 12. Group photo in Conference room*


*Jan 12. Group photo at reception*

### July 24

**Mr. Se Hwan Im** and **Ms. Ha Eun Doo**, Dept. of Mathematics, Daejin University, visited IKST to interview Dr. Seung Cheol Lee and Ms. Hye Soo Lee regarding the topics “How to prepare for $4^{th}$ Industrial Evolution as a job seeker” and “Job opportunities in India.”

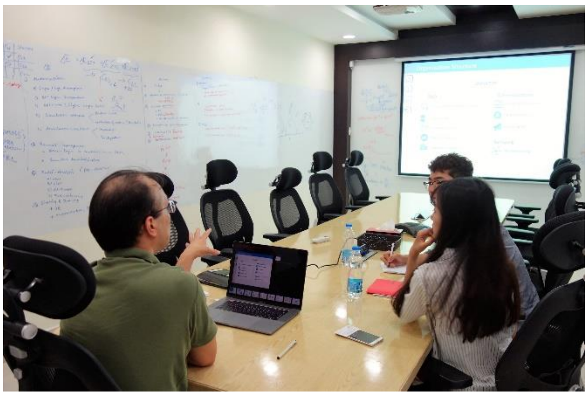

*July 24. Se Hwam Im and Ha Eun Doo conducted an interview with Dr. Seung Choel Lee.*

## October 12 & November 16

The **2017 Seoul Digitech High School Field Learning team**, including Se Hee Kim, Kang Hyun Lee, Hyun Seong Oh, Jong Gil Lee, Soo Jin Park, Min Ha Kim, Yae Seul Baek, Seung Jun Shon, Han Yi Jang, Beom Jun Kim, under the guidance of **Ms. Min Jeong Seo,** Digitech High School, and **Ms. Kyung Nam Seo,** Learning Lab Bengaluru, visited IKST to explore its facilities and activities.


*October 12. First team of students at IKST*

*November 16. Second team of students at IKST*

## Administration Staff

**Malini Sridhar**

*Head - Admin, External Affairs & Accounts*

Accountings, Visiting program, Networking support

malini.sridhar@ikst.res.in

**Venugopal K.**

*HR Manager*

HR management, Purchase, IT support

venugopal.kuruveri@ikst.res.in

**Hye Soo Lee**

*Coordinator - Logistics & PR*

KIST-IKST coordinating, PR activities, Survey research

coordination@ikst.res.in

## Finance

### Expenses Chart 2017

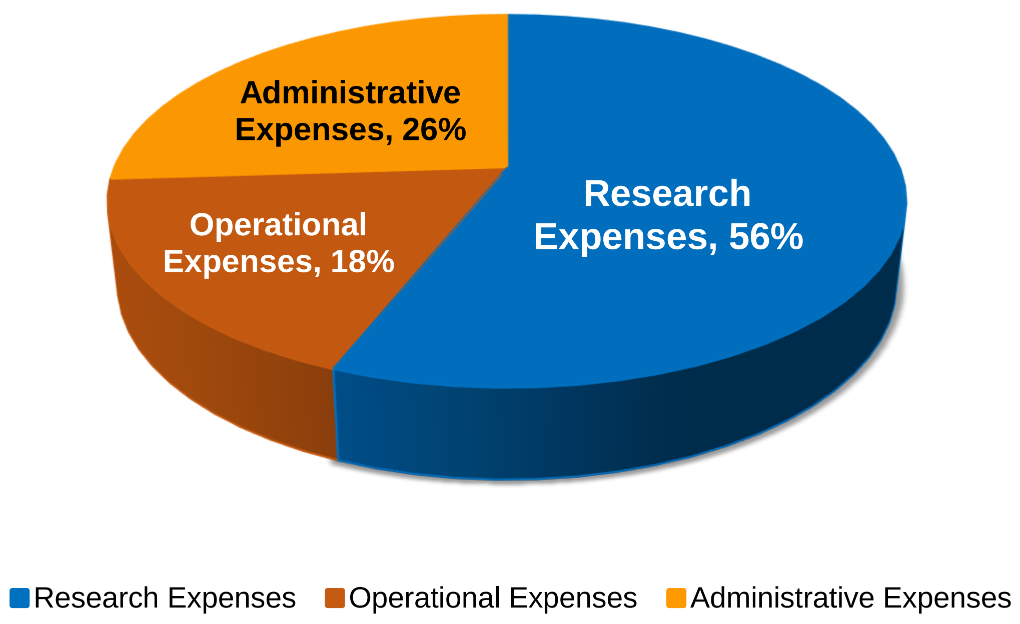


### Research Expenses Chart 2017

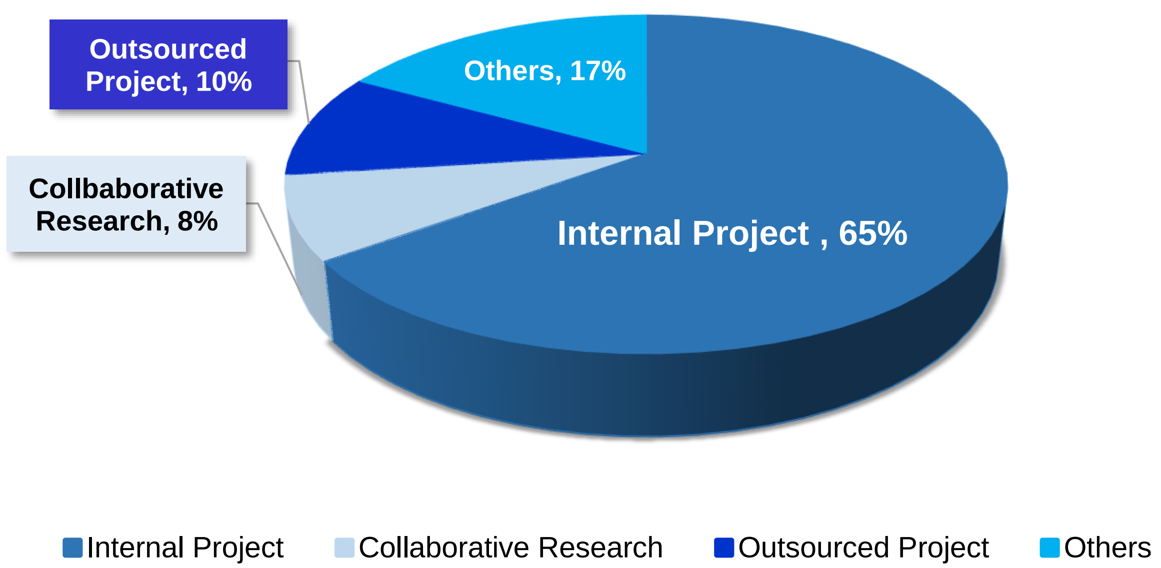

# IKST News

## 1. Dr. Seung Cheol Lee appointed as the head of center for the IKST

On January 1st 2017, Dr. Byeong Gwon Lee, the President of KIST, appointed Dr. Seung Cheol Lee as the head of center for IKST.

Dr. Lee received a Ph.D. from the Department of Metallurgical Engineering, Seoul National University, in 1999. He was an acting head of center for IKST from November 2014 till December 2016. During his time as an acting head, he put in considerable effort to help solidify IKST in India as a research organization and enhance R&D cooperation between India and Korea.

## 2. Internship to KIST, Seoul

Two students from IIT BBS were selected for the 2017 internship program and sent to the Center for Imaging Media Research, KIST, Seoul, South Korea.

## 3. Internal workshops

IKST held two half-yearly internal workshops on June 30th and December 20th in 2017. In the first half of the workshop, the employees presented the current status of their assigned jobs and their achievements and the Director gave them advice and suggestions for better performance. In the second half of the workshop, the employees reported their achievements throughout the year and their plans for the next year. The Director evaluated the performance of each person.

## 4. IKST holds joint workshop with IIT Bombay

From 10th to 12th January, 2018, IKST and IITB held a joint workshop on multiscale modeling at VMCC, IITB. Five Korean professors, 13 IIT professors, and four IKST researchers participated in the workshop.

## Cover Images

KIST campus in spring

KIST campus in winter

**Publisher**

Seung Cheol Lee

**Editor**

Hye Soo Lee

coordination@ikst.res.in

+91-80-4669-7016

**English Service**

Scholarly Editing and

Translation Services (SETS)

Indo-Korea Science and Technology Center

IKST, 3rd Floor, NCC Urban Windsor, Bengaluru, Karnataka 560043, India
Tel. +91-80-4669-7000
www.ikst.res.in

# 2018 Visiting Program to KIST

## A life time opportunity to visit the Republic of Korea

**IKST** calls for enthusiastic post graduate students to join the visiting program of the Korea Institute of Science and Technology (KIST).

**The Republic of Korea**, also known as South Korea, is the world's seventh largest advanced economy and fifth largest exporter with the G20's largest budget surplus and highest credit rating of any country in East Asia.

South Korea is the world's largest spender on R&D per GDP and the home of Samsung, LG, Hyundai, and Kia. South Korea has been named the world's most innovative country for four consecutive years, since 2014. It ranks first in business R&D intensity, manufacturing value addition, and patents filed per GDP. It ranks second in higher education efficiency and fourth in high-tech density.

KIST is the first government-established research institute in Korea and has led national economic development since the past 50 years. It has been ranked by Reuters as the World's Sixth Most Innovative Research Institute for two consecutive years, 2016 and 2017.

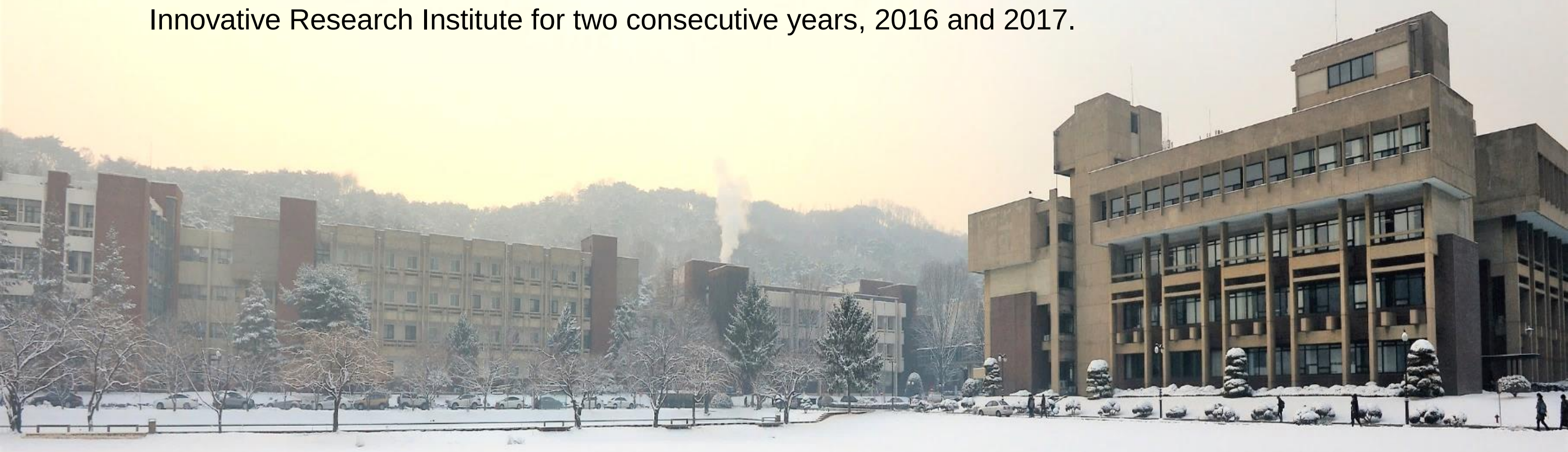

**Areas**

- Brain Science
- Biomedicine
- Green City Technology
- Post-Silicon Semiconductor
- Robotics and Media
- Materials and Life science
- Fuel Cell
- Clean Energy
- Sensor System and Hybrid Photoelectronics

For more details and to learn about our application process, visit the IKST website (www.ikst.res.in).